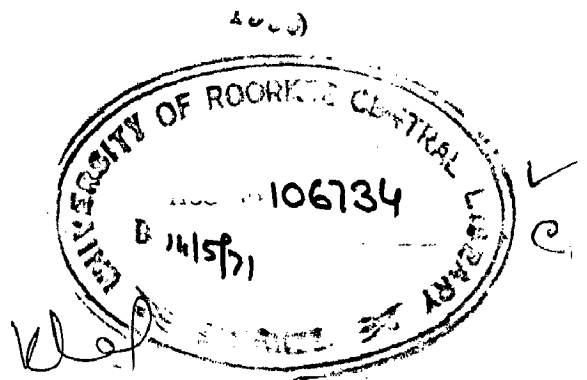


FLUME STUDIES ON RESISTANCE
OF TWO - DIMENSIONAL
STRIP ROUGHNESSES

A Dissertation
submitted in partial fulfilment
of the requirements for the Degree
of
MASTER OF ENGINEERING
in
HYDRAULICS AND IRRIGATION ENGINEERING

By

SUSHIL CHANDRA



DEPARTMENT OF CIVIL ENGINEERING
UNIVERSITY OF ROORKEE
ROORKEE
August 1970


CERTIFICATE

Certified that the dissertation entitled
 "FLUME STUDIES ON RESISTANCE OF TWO-DIMENSIONAL STRIP ROUGHNESSES"
 which is being submitted by Sri Sushil Chandra in partial fulfil-
 ment of the requirements for the award of the Degree of Master
 of Engineering in Hydraulics and Irrigation Engineering of the
 Roorkee University is a record of the student's own work carried
 out by him under my supervision and guidance. The matter
 embodied in this dissertation has not been submitted for the
 award of any other Degree or Diploma.

This is further to certify that he has worked for a
 period of seven and a half months from January 1970 to
 August 15, 1970 for preparing this dissertation for the Master
 of Engineering Degree at this University.

Roorkee

Dated: August 25, 1970


 (K.G. Rangaraju)
 Reader in Civil Engineering
 University of Roorkee,
 Roorkee, U.P.

ABSTRACT

This thesis presents the results of an experimental investigation on the mechanism of resistance to flow over artificial roughness elements. The studies were carried out on two-dimensional sharp-edged strips of negligible thickness placed on the bed of an open channel. The various aspects of the problem covered by the experiments included the resistance characteristics of a single roughness element as well as those of series of roughness elements placed on a smooth boundary. In case of elements in series, using two-dimensional strips having relative spacings of 60 and 80, the total resistance of the boundary, as well as the skin friction of the plane boundary were measured; the latter was measured using a Preston tube. Experiments were also performed to verify the hypothesis of Rangaraju and Garde that for roughness elements in series on a plane boundary, upto a relative spacing of 40, the negative friction in the standing eddy cancels with the positive friction further downstream and thus the net skin friction is zero. For this purpose experiments were made using two-dimensional strips placed on a boundary to which gravel particles were glued.

As a result of the present investigation it was proved that the above hypothesis is true upto a relative spacing of 40. In addition, information has also been presented about the form resistance of the strips and the skin friction of the plane boundary at relative spacings exceeding 40. Analysis of data on the drag of a single element has indicated a unique relation between the drag coefficient and the relative depth of flow.

ACKNOWLEDGEMENTS

The author wishes to express his deep sense of gratitude to his guide, Dr. K.G. Rangaraju, Reader in Civil Engineering, University of Roorkee whose expert guidance, invaluable suggestions, constant encouragement and keen interest thoroughly stimulated him in his work.

The author also takes this opportunity to thank the staff of Hydraulics Laboratory, University of Roorkee particularly Mr. B.R. Sethi and Mr. J.P. Jain for their wholehearted assistance and cooperation during the experimental work linked with the present investigation.

Last but not the least, the assistance of my colleague Mr. Ihsan Ahmad during the various stages of the work is gratefully acknowledged and appreciated.

CONTENTS

| <u>CHAPTER</u> | <u>DESCRIPTION</u> | <u>PAGE</u> |
|----------------|--|-------------|
| | LIST OF SYMBOLS | 5 - 8 |
| | LIST OF FIGURES | 9 - 10 |
| 1. | INTRODUCTION | 11 - 17 |
| 2. | REVIEW OF LITERATURE | 18 - 29 |
| 3. | ANALYTICAL CONSIDERATIONS | 30 - 38 |
| 4. | EXPERIMENTAL SET-UP AND PROCEDURE | 39 - 45 |
| 5. | ANALYSIS OF COLLECTED DATA | 46 - 67 |
| 6. | CONCLUSIONS AND SUGGESTIONS FOR FURTHER STUDY | 68 - 70 |
| | REFERENCES | 71 - 74 |
| | FIGURES | 75 - 98 |
| | APPENDIX | 99 - 102 |

LIST OF SYMBOLS

| <u>Symbol</u> | <u>Meaning</u> | <u>Units</u> | <u>Dimension</u> |
|---------------------------------|--|----------------|------------------|
| A | = Projected area of a body on a plane normal to direction of flow | m ² | L ² |
| B ₁ | = Constant in the resistance equation | Dimensionless | - |
| B | = Width of the channel | metres | L |
| C _D | = Drag coefficient with respect to Average velocity. | Dimensionless | - |
| C _{D0} | = Drag coefficient based on the average velocity but for infinite stream conditions | " | - |
| C _{D1} | = Drag coefficient based on the free stream velocity | " | - |
| C _{Dh} | = Drag coefficient based on the velocity at the crest level of the element. | " | - |
| C ₁ , C ₂ | = Constants in Resistance equation and function of L/h | " | - |
| C _f | = Local skin friction coefficient | " | - |
| C _{f1} | = Average friction coefficient assuming zero shear within standing eddy | " | - |
| C _{f2} | = Average friction coefficient for shear over a length L ₂ and defined by $C_{f2} = C_{f1} \cdot L_2/L$ | " | - |
| C _{f3} | = Average friction coefficient assuming skin friction to be effective in a length L ₃ | " | - |
| C _w | = Constant used by Morris | " | - |
| D | = Depth of flow in the flume measured from the bottom. | cms or m | L |

| <u>Symbol</u> | <u>Meaning</u> | <u>Units</u> | <u>Dimensions</u> |
|-----------------|--|-----------------------------|-------------------|
| d | = grain size | cms or m | L |
| d' | = Diameter of the Preston Tube | " | L |
| δ | = Thickness of the boundary layer defined so that the velocity at the edge of boundary is equal to 99% of the free stream velocity | cms | L |
| ρ | = Mass density of the flowing fluid | metric slugs/m ³ | ML ⁻³ |
| F _s | = Total positive skin friction between two roughness elements per unit width. | Kgm/metre | MT ⁻² |
| F' _s | = Total positive skin friction per unit width between 35 h and total length, L, between two roughness elements. | Kgm/m | MT ⁻² |
| F _r | = Froude's number of flow | dimensionless | - |
| f | = Darcy-Weisbach Resistance coefficient | " | - |
| f _s | = Darcy-Weisbach Resistance coefficient for smooth bed. | " | - |
| g | = Acceleration due to gravity | Metre/sec ² | LT ⁻² |
| h | = height of the roughness element | cms | L |
| j | = Width of groove in a bed with roughness elements | metres | L |
| K | = Karman's constant | dimensionless | - |
| K _s | = Equivalent sand grain roughness of the bed | metres | L |
| K' _s | = Resistance parameter and a function of roughness geometry | metres | L |
| L | = Spacing between the roughness elements | " | L |
| L ₁ | = length of the standing eddy | cms. | L |
| L ₂ | = L - L ₁ | cms. | L |
| L ₃ | = L - 35 h (h in metres) | metres | L |

| <u>Symbol</u> | <u>Meaning</u> | <u>Units</u> | <u>Dimensions</u> |
|---------------|---|---|-------------------------------|
| λ | = Roughness concentration, defined as the ratio of projected area of the roughness elements to the area of the bed. | dimensionless | - |
| μ | = Dynamic viscosity of the flowing fluid | $\frac{\text{kgm-sec}}{\text{metre}^2}$ | $\text{ML}^{-1}\text{T}^{-1}$ |
| N | = No. of elements in periphery | dimensionless | - |
| n | = Manning's coefficient | $\text{metre}/\text{sec}^{-1/3}$ | $\text{TL}^{-1/3}$ |
| ν | = Kinematic viscosity of the flowing fluid | $\text{m}^2/\text{sec.}$ | L^2T^{-1} |
| p_u | = Pressure on the upstream face of the roughness element at a height y from the floor | Kgm/m^2 | $\text{ML}^{-1}\text{T}^{-2}$ |
| p_d | = Constant pressure on the downstream face of the element | " | " |
| P | = Wetted Perimeter of the channel | metres | L |
| R_b | = Hydraulic Radius of the bed of the channel | " | " |
| Q | = Discharge flowing | m^3/sec | L^3T^{-1} |
| R_e | = Reynolds No. of flow | Dimensionless | - |
| R_h | = Reynolds No. with respect to the velocity at the crest of the element | " | - |
| R_x | = Reynolds number of flow at a distance x from the edge of the plate | " | - |
| γ | = Unit weight of the flowing fluid | Kgm/m^3 | $\text{ML}^{-2}\text{T}^{-2}$ |
| r_o | = Radius of the conduit | metres | L |
| Δp_p | = Preston tube reading (difference between static pressure and Pitot pressure) | cms. | L |
| ΔF | = Force per unit width on the element | Kg/m | ML^{-1} |
| S | = Water surface slope | Dimensionless | - |

| <u>Symbol</u> | <u>Meaning</u> | <u>Units</u> | <u>Dimensions</u> |
|---------------|---|--------------------|----------------------------------|
| S_1 | = Peripheral spacing between roughness elements | metres | L |
| t | = thickness of roughness element | cms | L |
| τ_0 | = Total shear stress on the bcd of the channel | Kgm/m ² | ML ⁻¹ T ⁻² |
| τ'_0 | = Skin friction at a distance x from the element | " | " |
| τ'_{01} | = Average shear stress due to the skin friction of the plane boundary when the shear in standing eddy is neglected. | " | " |
| τ''_{01} | = $\tau_0 - \tau'_{01}$ | " | " |
| τ'_0 | = net positive friction of the plane boundary which is equal to the friction between $33h$ and L . | " | " |
| τ''_0 | = $\tau_0 - \tau'_0$ | " | " |
| V_0 | = free stream velocity | metres/sec | LT ⁻¹ |
| U_h | = Velocity of height 'h' from the floor | " | " |
| U | = velocity at a height 'y' from the floor | " | " |
| V | = Average velocity in the vertical centre line of the channel | " | " |
| \bar{V} | = Average velocity over the cross-section of the channel | " | " |
| V_* | = Shear velocity = $\sqrt{\tau_0/\rho}$ | " | " |
| x | = distance along the flow | cms | L |
| X^*, Y^* | = Parameters used by Patel | Dimensionless | - |
| y | = Height measured from the floor | metres | L |

LIST OF FIGURES

| <u>Fig.No.</u> | <u>Description</u> |
|----------------|---|
| 2.1 | Variation of C_{D_0} with δ/h for normal plates in boundary layer (Ref. 18). |
| 2.2 | Variation of C_1 with L/h for Two-Dimensional elements in series (Ref.19). |
| 2.3 | Variation of C_2 with L/h for two-Dimensional elements in series (Ref.19). |
| 2.4 | Transition functions for conduit roughened with cubes (Ref.3). |
| 2.5 | Plot of C_{D_h} vs. R_h (Ref. 3). |
| 3.1 | Schematic diagram of shear stress distribution |
| 4.1 | Schematic diagram of experimental flume. |
| 5.1 | Pressure difference around single element. |
| 5.2 | Variation of $1/\sqrt{C_D}$ with $\log_{10} D/h$ for single element |
| 5.3 | Variation of C_D with D/h for single element. |
| 5.4 | Pressure difference around elements in rough boundary. |
| 5.5 | Comparison between τ_0 and τ_0^* for rough boundary with strips. |
| 5.6 | Variation of $1/\sqrt{C_D}$ with D/h and L/h for Elements in series. |
| 5.7 | Variation of \bar{V}/V_* with R_D/h and L/h for Elements in series. |
| 5.8 | Variation of U/V_* with $\log_{10} y/h$ for elements in rough boundary. |
| 5.9 | Variation of U/V_* with $\log_{10} y/h$ for elements in rough boundary. |
| 5.10 | Variation of \bar{V}/V_* with $\log_{10} R_D/h$ and L/h for smooth boundary. |

| <u>Fig.No.</u> | <u>Description</u> |
|----------------|---|
| 5.11 | Variation of C_f with x/L and x/h for elements on smooth boundary. |
| 5.12 | Variation of C_f with $\frac{\bar{V}_R}{V}$ for elements on smooth boundary. |
| 5.13 | Variation of C_{f_1} with \bar{V}_{R_1}/V for elements on smooth boundary. |
| 5.14 | Variation of C_{f_2} with \bar{V}_{R_2}/V for elements on smooth boundary. |
| 5.15 | Variation of C_{f_1} with \bar{V}_L/V for elements on smooth boundary. |
| 5.16 | Variation of C_{f_2} with \bar{V}_L/V for elements on smooth boundary. |
| 5.17 | Variation of C_{f_3} with \bar{V}_{R_3}/V for elements on smooth boundary. |
| 5.18 | Variation of C_{f_3} with \bar{V}_L/V for elements on smooth boundary. |
| 5.19 | Variation of L_1/h with \bar{V}_{R_1}/V for elements on smooth boundary. |
| 5.20 | Variation of $\frac{1}{\sqrt{C_D}}$ with $\log_{10} D/h$ and L/h for elements on smooth boundary. |
| 5.21 | Variation of C_1 with L/h for elements on smooth boundary |
| 5.22 | Variation of C_2 with L/h for elements on smooth boundary |
| 5.23 | Variation of T'_0/T_0 with L/h for elements on smooth boundary. |
| 5.24 | Prediction of shear for Basha's data using author's method. |
| 5.25 | Variation of U/V with $\log_{10} y/h$ for elements in smooth boundary. |
| 5.26 | Variation of U/V with $\log_{10} y/h$ for elements in smooth boundary. |

CHAPTER - 1

INTRODUCTION

1.1 Preliminary Remarks:

The problem of resistance to flow in open channels has received the attention of hydraulic engineers for a long time because of its importance in several practical problems. Knowledge of the resistance to flow is important in the design of channels, preparation of stage - discharge curves and in the computation of sediment transport rate in alluvial channels. However, in spite of the vast amount of work done on the problem, the resistance for different roughnesses under different flow conditions is not accurately known at present. Consequently correct solution of the problems mentioned earlier is also not possible.

The commonly used resistance relations are those of Chezy and Manning. In both of these equations the resistance coefficient is taken constant for a particular type of roughness, regardless of fluid and flow conditions. However this is seldom true in case of natural channels and, therefore, those equations are inadequate in describing the behaviour of such channels over a wide range of flow conditions.

1.2 Studies on Artificial Roughnesses:

With the object of providing a roughness standard for

open channels similar to Nikuradse's sand-grain concept for commercial pipes, several studies have been carried out using artificial roughness elements. Contributions of Powell (16), Johnson (8), Soyro - Albertson (24), and Adachi (1) are worth mentioning in this connection. These investigators studied the total resistance of a boundary with various types and concentrations of roughness elements. However these studies have not led to an acceptable roughness standard for open channels.

Einstein and Banks (4), by a rational analysis based on flume studies with various patterns of roughness elements, concluded that the total resistance of the boundary having a series of roughness elements on it can be taken as sum of the resistance of individual roughness elements. In other words presence of a roughness element has no significant effect on the resistance of other roughness elements and the total resistance can be obtained as the sum of form resistance of individual roughness elements and the boundary friction over the whole area. Based on this concept Einstein and Barabeno (5), proposed a method for prediction of resistance to flow in alluvial channels. However because of infinite arrangements and spacings of roughnesses that are encountered in natural channels the interference effect may become important and needs to be investigated properly.

Rangaraju and Gardo (19), made a thorough investigation

of the effect of interference on the resistance of artificial roughness elements by conducting extensive experiments in a flume as well as in wind tunnels. They used sharp-edged two-dimensional strips of negligible thickness as the roughness elements on a smooth plane boundary. Their conclusions were that the total resistance of a plane boundary with roughness elements having relative spacing between 2.5 and 40 can be estimated on the assumption that the total resistance is equal to the form resistance of the roughness elements; the form resistance of the strips is strongly dependent on the relative spacing and the ratio of depth of flow to height of element. This means that, in the range of their experiments, the skin friction is practically zero. One can arrive at such a conclusion if the skin friction of the plane boundary is a very small fraction of the total resistance; because of the smoothness of the boundary in such a case the total resistance would prove equal, within range of experimental accuracy, to the measured form drag as found by Rangaraju and Gardo. The net skin friction can also be nearly zero (for L/h less than 40) if the positive friction beyond the standing eddy downstream of the roughness cancels out with the negative friction within the eddy. Such an assumption has been made by Rangaraju and Gardo in their studies. However in the absence of measurements of skin friction for the runs conducted by Rangaraju and Gardo, it is not possible to say which of the above hypotheses

is correct. The foregoing point can be settled convincingly if the plane boundary between the roughness elements is made quite rough. If the hypothesis of Rangaraju and Gardé that the net skin friction is zero for $L/h < 40$ (where L is spacing between roughness elements and h is the height of elements) is true the total resistance of the roughened plane bed on which roughness elements are placed should prove equal to the total resistance of the smooth plane bed with the same roughness geometry provided $L/h < 40$. On the other hand, if the resistance in the former case exceeds that in the latter, the conclusion of Rangaraju and Gardé that the total resistance is equal to the form resistance of the strips (for $L/h < 40$) may not be acceptable.

1.3 Scope of Present Investigation:

The present investigation was, therefore, carried out to test the validity of the assumption discussed above and also to extend the results of Rangaraju and Gardé to larger spacings of roughness elements. For the former purpose resistance studies were made using two-dimensional strips placed on a plane boundary on which were glued gravel particles of 2 mm size. These studies were performed for two values of L/h viz. 20 and 40 - the latter being the limit upto which there is no net skin friction, according to Rangaraju and Gardé.

At L/h values greater than 40, the net skin friction of the plane boundary is expected to be significant. Hence studies were carried out for L/h values greater than 40, using two-dimensional strips placed on a smooth boundary. These studies included the measurement of skin friction by a Preston Tube.

For the case of a single two-dimensional sharp-edged roughness element placed on a plane boundary the available information is based mainly on the wind tunnel studies made by Plato (15), Good and Joubert (6) and Rangaraju and Gardo (18). An attempt at extending these results to open channel flow (18) proved unsuccessful, probably because of the influence of the free surface. Hence one aspect of the study was to provide information on the resistance of a single element placed on a plane boundary. It may be noted that this forms a limiting case of a series of elements placed on the boundary.

1.4 Limitations of Study:

The experiments were performed on two-dimensional sharp-edged roughness elements of negligible thickness placed on the bottom of the flume and extending across the entire width.

The work was carried out in three parts:

- (a) To study the resistance of a single isolated roughness element placed on the boundary. Two sizes of element viz 3 cm and 4 cm were used to cover a range of D/h from 2.0 to 12.0.

- (b) To study the resistance characteristics for a series of roughness elements placed on a smooth boundary for large spacings viz $L/h = 60$ and $L/h = 80$. The height of roughness in this case was kept as 1 cm.
- (c) To study the resistance to flow over strip roughnesses placed on a plane gravel bed. Using a roughness of 4 cm height, two different spacings ($L/h = 40$ and $L/h = 20$) were used in this part of the study.

The experiments were, in all cases, restricted to low froude numbers.

CHAPTER - 2

REVIEW OF LITERATURE

2.1 Preliminary Remarks

Considerable work has been done during the last three decades concerning the resistance to flow in rigid boundary open channels. Using artificial roughnesses on the channel boundary. These studies have been performed using different types and arrangements of roughness elements. The salient features of some of these investigations are discussed in the following paragraphs. For the present study the review of literature has been divided into two parts:

- (a) Studies on resistance of single roughness element kept either on the bottom of an open channel or on the wind tunnel floor.
- (b) Studies on resistance of series of roughness elements placed on the bed of an open channel.

2.2 Studies on Single Roughness Element:

Plato (13), 1964, studied the problem of drag on a smooth boundary having a two-dimensional sharp-edged normal plate immersed in its turbulent boundary layer. The experiments were performed in a wind tunnel having a 1.83 m square section. The height of plate was varied from 1.25 cm to 5.00 cm and variation of the drag coefficient with δ/h was studied. (δ being thickness

of the boundary layer). The main conclusions obtained as a result of his investigation were:

- (a) drag coefficient C_{D_1} of the roughness element was related to δ/h by the equation,

$$C_{D_1} = 1.03 (h/\delta)^{2/7} \quad (2.1)$$

where, C_{D_1} = Drag coefficient of the plate with respect to free stream velocity.

- (b) The negative friction in the standing eddy zone cancels the positive friction downstream of reattachment point over a distance 33 times the height of roughness element. Beyond this point, theory of undisturbed boundary layer is applicable.

Adachi (1), 1964, conducted open channel studies using a two-dimensional wooden bar 5 mm high and 6.4 mm thick placed on the channel bed. He measured the form drag of the strip under various depths of flow. The tests were carried out in a 20 cm wide, 30 cm deep and 14.40 meters long steel flume having a slope of 1/500. He argued that in case of roughness element placed on the channel bed, the velocity gradient over the element height is marked and accordingly the average velocity needs to be taken as the characteristic velocity. The relative depth D/h , was found to be a significant parameter and to affect the drag coefficient defined with respect to average velocity.

Consequently he plotted C_D against D/h and the curve proposed by Adachi has been shown in Figure (3.3).

Good and Joubert (5), 1968, made an experimental study on the drag coefficient of a two-dimensional normal plate immersed in a turbulent boundary layer. The experimental brass plate forming the smooth boundary was 6" wide and 3 ft 7" long. The height of normal plate was varied from 1" to $4\frac{1}{2}$ " by firmly clamping it to a 6" wide panel. The results showed that the drag coefficient of the plate is related to dimensionless parameter V_* / V_0 except possibly when $h/\delta < 1$, in accordance with the relation,

$$C_{D1} = f(h/\delta, V_*/V_0) \quad (2.2)$$

where, V_0 = free stream velocity

and V_* = shear velocity

It was further found that over a considerable range of plate heights C_{D1} varies logarithmically with h/δ , the slope of semi-log plot being different for different V_*/V_0 . They also compared their data with Plato's data and found the agreement good.

Chang (3), 1970, carried out detailed investigations of the relationship between friction factor of flow over ripple beds and geometric properties of ripples such as shape and concentration. During this study, he studied the length of standing eddy behind a two-dimensional normal plate placed on the channel bed. He found that L_1/h is a function of $\bar{V}D/\nu$. Fig.(3.19) shows the variation of L_1/h with $\bar{V}D/\nu$ for runs

in the range of experiments, performed by them the resistance could be predicted by using standard values (22) of drag coefficient.

This concept implied that the interference effect is not significant. However while dealing with small spacings and various types of roughnesses one can still expect the interference effect and this aspect needs further investigation.

Morris (11), 1955, presented a new concept of flow over rough pipe and channel surfaces based on the effect of longitudinal spacing of roughness elements. He expressed the opinion that longitudinal spacing of the elements is a roughness dimension of paramount importance in rough conduits. He classified the flow over rough surfaces into three categories:

- (a) Isolated roughness flow: In this type of flow wake zone at each element is fully developed and dissipated before the next element is reached. For this zone equation of friction factor was given as,

$$f = f_s \left(1 + \frac{67.2 C_D}{L/h} \left(1 - \frac{NS_1}{P} \right) \right) \quad (2.4)$$

where, f_s = friction factor for plane boundary at Reynold's

No. of flow

N = no. of elements in periphery

S_1 = clear peripheral spacing between elements

and P = wetted perimeter.

- (b) Wake interference flow: In this case spacing of elements is such that the wake zones behind each element are not fully dissipated before the next element is reached. For this type of flow he found that,

$$\frac{1}{\sqrt{f}} = 2 \log_{10} \frac{D}{L} + 1.75 \quad (2.5)$$

- (c) Quasi-Smooth flow: When roughness elements are so close that the flow skims over the crest of each element and stable vortices exist between various elements the flow was termed as quasi-smooth. For this type of flow Morris gave the following equation for the friction factor,

$$f = f_s + \left(\frac{C_w U_h}{\bar{V}} \right)^2 / \frac{L}{h, j} \quad (2.6)$$

where, U_h is the velocity at the crest level of element

C_w = constant (taken as 0.5)

j = width of groove

In the equation (2.6) either h or j , whichever is smaller is to be used.

Sayre and Albertson (21), 1961, carried out flume studies on discontinuous angle iron roughness elements with different spacings and studied the variation of K'_s (roughness parameter) with pattern of roughness. They suggested the resistance equation as

$$\frac{\bar{V}}{\bar{V}_*} = 6.06 \log_{10} \frac{D}{K'_s} \quad (2.7)$$

The above equation yield a value of Karman's constant (K) as 0.38, however analysis of velocity profiles revealed that K changes appreciably with roughness concentration. Nevertheless, they recommended K is equal to 0.38 for wake interference flow.

From the study of variation of K'_s with the roughness pattern they found that for different arrangement and type of roughness elements maximum resistance could occur at various concentrations.

O' Loughlin and Macdonald, 1964, performed open channel experiments and investigated the effect of roughness pattern and concentration on the resistance coefficient. They found that shape and pattern of roughness elements has no significant effect on the resistance coefficient below a concentration of 0.10. But above this value of concentration resistance coefficient is affected considerably by the concentration.

O'Loughlin (26), 1965 assumed that the departure from the logarithmic profile can be expressed by defining a momentum diffusion coefficient ϵ' , such that,

$$\epsilon' = \epsilon_{\log} + \epsilon_w \quad (a)$$

The velocity profile is a combination of a logarithmic field and a mixing effect in the wake layer.

$$\text{Here } \epsilon_{\log} = \frac{\tau}{\left(\frac{du}{dy}\right)_{\log}} \quad (b)$$

$$= \frac{\tau y}{\rho A V_*} \quad (c)$$

ϵ' was assumed constant between the boundary and a level $y = 0.2D$ which is comparable to roughness height i.e. ϵ_w will be negligible above this level and ϵ' will be equal to ϵ_{\log} . Assuming such a distribution of ϵ' , he obtained the velocity distribution for flow over a boundary with cubes placed at a regular spacing. He found that the actual profiles showed qualitative agreement with the theoretical profiles.

He also studied the variation of τ'_{o_1}/τ_o with D/h and roughness concentration as predicted by his mathematical model.

Here τ'_{o_1} = Average shear stress of the boundary between the roughness elements.

and τ_o = Total shear stress.

The experimental values were found to be lower than this. For cubes with concentration $y = 1/256, 1/128, \text{ and } 1/64$, the values of τ'_{o_1}/τ_o were found to be 0.60, 0.50 and 0.42 respectively, for the D/h value used by him.

Rangaraju and Gardo (19), 1970, carried out investigations of the interference effect on the resistance of two-dimensional strip roughness at different spacings. They found that the total resistance of a plane boundary having series of roughness elements with L/h between 2.5 and 40 can be assumed equal to form resistance of the roughness elements. Based on flume and tunnel data, an empirical equation for computing the drag was given as

$$\frac{\lambda}{\sqrt{C_D}} = C_1 \log_{10} \frac{D}{h} + C_2 \quad (2.8)$$

where C_1 and C_2 are constants and functions of L/h . The variations of C_1 and C_2 with L/h are shown in Fig.(2.2) and (2.3) respectively.

Rangaraju and Gardo also showed by plotting of data that the method given by Morris (11) does not yield satisfactory results over a wide range of data.

Roberson and Chen (20), 1970, investigated the flow in conduits with low concentration with regularly spaced cubes and spheres so as to obtain functional relationship between concentration of given type of roughness and resistance produced by this roughness. They developed a procedure for obtaining transition functions for flow in conduits roughened with discrete elements, assuming a logarithmic velocity distribution with a suitable correction for the 'wake effect'. The drag characteristics of roughness elements, viscous resistance of the

smooth wall and velocity distribution conduit were considered separately and equations relating these were solved to obtain a resistance relation. The plots of transition functions for different concentration ranging from 0.0001 to 0.123 as well as curves of coefficient of drag against Reynolds number were also plotted. These curves for cubical roughnesses are shown in Figures (2.4) and (2.5).

A comparison was also made of the data of this analysis with the experimental results of Kolosov and O'Loughlin as shown in Figure (2.4). This indicates reasonably good agreement between theory and experiments.

Drag coefficient values computed with respect to u velocity over the height of the roughness element (cube or sphere) were found to be independent of the nature of velocity distribution.

Besides these investigations discussed above, several other investigations have been carried out by Kolosov (9), Peterson and Mohanty (14), Rouse, Kolosov and Davidian (23), Horblich and Shulitz (7) using artificial roughness elements. These have not been reviewed here, since they are not directly related to the work planned in this study.

Summary

Among the various investigations on the subject of artificial roughness, the studies of Rangaraju-Gardo and Fabercon and Chen are the only ones dealing with the individual roughness

effects and may be said to be based on the ideas put forward by Einstein and Benke. It is interesting to note that the studies of Rangoraju and Garde were performed at fairly high concentrations using two-dimensional strips. As such they were concerned with the variation of the form drag coefficient of the strips with their geometry; the skin friction of the plane boundary was found to be practically nil. On the other hand, Roberson and Chen performed their experiments using cubes at low concentration. Therefore, the skin friction of the plane boundary was found to be a significant part of the total resistance and the premise that C_{Dh} is independent of velocity distribution was found to be valid for the low concentrations studied by them. In a general case, one would possibly be required to consider the skin friction of the plane boundary as well as the variation of the form drag coefficient of the roughnesses with the relative spacing. Such an approach is planned during this investigation.

CHAPTER - 3

ANALYTICAL CONSIDERATIONS

3.1 Preliminary Remarks:

Having considered the work of past investigators on the problem of resistance, some basic aspects of the problem are discussed in this Chapter. This would serve as a guideline for the subsequent analysis of the data of the present investigation.

3.2 Drag Coefficient:

It is well known that a body placed in a fluid flowing at uniform velocity past it experiences a force in the direction of flow which is termed as drag force. The body, in turn, exerts a force equal in magnitude but opposite in direction. This is commonly known as resistance. The total drag on the body is the sum of deformation drag, friction drag and form drag. Deformation drag is due to wide spread deformation and occurs only at low Reynold numbers. Friction drag is caused by the shear stress due to the velocity gradient near the body and is a function of Reynold's number. The form drag, on the other hand is due to pressure difference between the front and rear of the body caused as a result of separation of flow. In case of two-dimensional sharp-edged strips kept in a fluid where Reynold's number exceeds 10^5 only form drag is prevalent, the extent of which

is not known for various geometries. In the case of a plane boundary with a regular array of two-dimensional strips total drag is equal to the drag on the strip plus the drag of the plane boundary. Since no theoretical method is available for estimation of form drag on normal strips placed on the boundary at different spacings, experimental investigations are the only solution. Also estimation of frictional resistance of the plane boundary by theoretical methods is complicated because of the presence of separation zone and the ill-defined characteristics of the redeveloping boundary layer. Hence the convenient way to tackle the problem is to resort to experimentation. The present study is, therefore, planned to provide experimental data on the form drag of strips and the skin friction of the plane boundary at various spacings. In this Chapter dimensional analysis of the problem has been carried out to facilitate analysis of the experimental data. Also some basic ideas resulting from past investigation's have been introduced to obtain equations which would form the starting point for analysis of data.

3.3 Resistance of a Single Element:

The force ΔF on a unit width of a two-dimensional normal plate kept on the boundary of an open channel can be described by the following functional relation:

$$\Delta F = \phi (h, D, V, \rho, \mu, g) \quad (3.1)$$

where ρ is the mass density, μ - dynamic viscosity of the flowing fluid and g - acceleration due to gravity.

By choosing V , h and ρ as repeating variables the above equation can be rewritten in dimensionless form as,

$$\frac{\Delta F}{\rho \frac{V^2}{2} \cdot h} = \phi_1 \left(D/h, \frac{Vh\rho}{\mu}, \frac{V}{\sqrt{gh}} \right) \quad (3.2)$$

$$\text{i.e. } C_D = \phi_2 \left(D/h, \frac{Vh\rho}{\mu}, \frac{V}{\sqrt{gh}} \right) \quad (3.3)$$

For sharp - edged roughness elements kept in a uniform stream the drag coefficient is known to be independent of Reynold's number of values of Reynold's number above 10^5 . Assuming that this is valid for elements on the boundary also, Equation (3.3) can be simplified for $R_e > 10^5$ as,

$$C_D = \phi_3 \left(D/h, \frac{V}{\sqrt{gD}} \right) \quad (3.4)$$

The Equation (3.4) gives the functional relationship of the drag coefficient of an isolated roughness element placed on the bottom of the flume. The variation of C_D with both these parameters will be studied in the present investigation.

3.4 Resistance of a Plane Boundary Glued with Gravel and Two-Dimensional Strips:

The second aspect of the experimental programme is to measure the resistance characteristics of a plane boundary with gravels of 2 mm size glued on it, two-dimensional strips being fixed on this surface at the desired spacing. It is intended to determine the total resistance of the boundary as well as the form drag coefficient of the strips by pressure measurements.

The functional relationship for the total resistance of the boundary can be written as,

$$S' = \phi_4 (\bar{V}, D, \rho, \mu, g, h, d, L) \quad (3.5)$$

where, d = grain size.

Choosing, \bar{V} , D and ρ as repeating variables,

$$S' = \phi_5 \left(\frac{\bar{V}}{\sqrt{gD}}, \frac{Vh\rho}{\mu}, D/h, D/d, L/D \right) \quad (3.6)$$

This can be modified as,

$$\frac{\bar{V}}{V_*} = \phi_6 \left(\frac{\bar{V}}{\sqrt{gD}}, \frac{Vh\rho}{\mu}, D/h, h/D, L/h \right) \quad (3.7)$$

At low Froude's number resistance coefficient is independent of Froude's number as found by Koloscuo (9). Hence $\frac{\bar{V}}{\sqrt{gD}}$ can be omitted. Further $\frac{Vh\rho}{\mu}$ can also be ignored for $Re > 10^5$.

h/d remained constant during the study, hence Equation (3.7)

simplifies to,

$$\frac{\bar{V}}{V_*} = \phi_7 (D/h, L/h) \quad (3.8)$$

Using the hydraulic radius with respect to the bed of the flume, R_b , the foregoing equation becomes,

$$\frac{\bar{V}}{V_*} = \phi_8 (R_b/h, L/h) \quad (3.9)$$

Similarly the drag coefficient of the strip can be written as,

$$C_D = \phi_9 (D/h, L/h) \quad (3.10)$$

3.5 Resistance of a Smooth Boundary with Two-Dimensional Strips Placed on It:

In this aspect of the study it is proposed to use two-dimensional strips of 1 cm height placed at the desired spacing along the length of the flume. The total resistance of the bed as well as the skin friction of the plane boundary would be measured. From these it is proposed to estimate the form resistance of the strips as pressure measurement on a strip of such a small height would be very difficult.

For the total resistance of the boundary, one can write the functional relation,

$$S' = \phi_{10} (\bar{V}, D, \rho, h, \mu, g, L) \quad (3.11)$$

This can be simplified to,

$$\frac{\bar{V}}{V_*} = \phi_{11} \left(R_b/h, L/h, \frac{\bar{V} R_b \rho}{\mu} \right) \quad (3.12)$$

after omission of Froude's number which is very low in the present experiments.

In general the average bed shear stress, τ_0 , can be written as sum of the shear due to the roughness elements and the net shear due to the skin friction of the plane boundary. It may be noted that within the separation zone downstream of each element, there is reverse flow at the bed and hence the shear is negative. Downstream of the standing eddy, the shear is once again positive. Hence two approaches are open for analysis of the skin friction data and the computation of the form drag of the roughness elements.

I Approach: When the negative shear in the standing eddy is completely neglected, assuming the reverse velocities to be too low to cause any shear.

II Approach: When it is assumed that the negative shear in the zone of standing eddy cancels with the positive shear over a certain distance from the boundary. Further analysis will be carried out based on both these approaches.

3.5.1 I Approach:

If negative friction is completely neglected then, total shear can be written as,

$$\tau_o = \tau'_{o_1} + \tau''_{o_1} \quad (3.13)$$

where τ'_{o_1} is the average shear stress due to the skin friction of the plane boundary (See Fig.(3.1)).

and τ''_{o_1} = shear stress due to form resistance of roughness elements.

τ'_{o_1} may be written as,

$$\tau'_{o_1} = C_{f_1} \frac{\rho V_o^n}{2} \quad (3.14)$$

and τ''_{o_1} may be written as,

$$\tau''_{o_1} = C_{D_1} \frac{h}{L} \frac{\rho V_o^n}{2} \quad (3.15)$$

Equations (3.13), (3.14) and (3.15) will form the basis of analysis of data using this approach.

3.5.2 II Approach:

Plato (15), in his study of a normal plate placed in a turbulent boundary layer, found that the net friction of the plane boundary for a distance of 33 times the height of the plate from the plate is zero. Apparently, within this distance,

the negative friction within the standing eddy compensates for the positive friction downstream of the eddy. Similar results are not available for fully developed flow in an open channel on which a series of roughness elements are placed. However using Plato's criterion for this case also, as a first approximation, one can write

$$\tau_o = \tau_o' + \tau_o'' \quad (3.16)$$

where τ_o' is the effective or net positive friction of the plane boundary (See Fig.(3.1)).

τ_o' and τ_o'' may be written as

$$\tau_o' = C_{f_3} \rho \frac{V^2}{2} \quad (3.17)$$

$$\text{and,} \quad \tau_o'' = C_D \cdot h/L \cdot \rho \frac{V^2}{2} \quad (3.18)$$

Equations (3.16), (3.17) and (3.18) will form the basis for analysis of data using this approach. On the basis of dimensional analysis presented earlier, one can write

$$C_{f_1} \cdot C_{f_3} = \phi \left(\frac{\bar{V} R_b \rho}{\mu}, L/H, R_b/h \right) \quad (3.19)$$

$$\text{and,} \quad C_D \cdot C_{D_1} = \phi (D/h, L/h) \quad (3.20)$$

CHAPTER - 4

EXPERIMENTAL SET-UP AND PROCEDURE

4.1 Preliminary Remarks:

All the experiments concerning the present investigation were conducted in the Hydraulics Laboratory of the University of Roorkee, Roorkee. The work was programmed and executed as to provide detailed information regarding the various parameters required for further analysis as discussed in the preceding Chapter. The experiments were performed in three parts viz. experiments on the single isolated roughness element placed on the bottom of the flume, studies on series of roughness elements with rough boundary and series of elements placed on a smooth boundary. The details of these experiments, various equipment used and the procedure followed are discussed in various sections of this Chapter.

4.2 Details of Equipment Used:

The experimental work was done in a 47.25 cm wide, 60 cm deep and 11 meters long tilting flume with glass side walls and a wooden false bottom^(Photo-1). The flume was of the recirculating type with an overhead tank and sump arrangement. It was provided with adjustable brass rails on the top of each side wall and these were maintained parallel to the bed. The pointer gage was mounted on a wheeled carriage which could be moved on the

rails. A tail gate was provided at the downstream end of the flume for adjusting the depth of flow.

The discharge was measured by a calibrated rectangular sharp-crested weir installed in a tank downstream of the flume. The velocity distribution in the flume during a run was measured by a calibrated prandtl tube. The ensuing heads were read on an inclined manometer.

Pressure measurements in case of single element and elements in rough boundary were made using a sharp-edged element of wood, 0.30 cm thick but chamfered at the top to get a knife edge. Pressure taps were provided approximately 5 mm apart both on upstream and downstream faces of the element, but very close to the centre of its width. Plastic tubes were connected to the pressure taps and led to the limbs of an inclined manometer.

For studies on series of elements angle iron strips of negligible thickness were nailed to flume bottom at the required spacing to form the roughness. The elements spanned over the full width of the flume in all the runs carried out during this study.

4.3 Experimental Procedure (Single Roughness Element):

For the study of the variation of drag on a single normal plate kept on the boundary the two-dimensional wooden strip of

the required height was nailed to the flume bottom at a distance 5.5 m from the upstream end of the flume. For any particular discharge, the required depth of flow upstream of the element was obtained by adjusting the tail gate. The pressures on the two faces of the element were then measured.

Velocity profile at the centre line of width was taken 50 cm upstream of the element with a calibrated prandtl tube. Flow depth for each run was measured by a pointer gage having a least count of 0.01 cm. The temperature of the flowing water and the discharge were also recorded.

The experiments were performed using strips of two heights, viz 3 cm and 4 cm. A total of 14 runs covering range of depth from 7.50 cm to 36.00 cm were made for this study.

4.4 Experimental Procedure (Series of Elements on a Rough Boundary):

In order to have a rough boundary gravel of size 2 mm was glued uniformly to bottom of the flume. The roughness elements used in this part of study were angle iron strips of galvanised iron 4 cm in height, ^(see Photo-2) One roughness element near the middle of length of flume was made of wood and provided with pressure taps to facilitate pressure measurement. The experimental work was done on two slopes 1×10^{-3} & 2×10^{-3} . For each slope two different roughness patterns, of spacing 80 cm and 160 cm were used. After the required roughness pattern was placed on the flume at the desired slope, uniform flow was

established at pre-determined depth and the discharge and temperature were measured. On each slope three different depths were used for each roughness pattern. For each run two velocity profiles were taken, midway and quarterway between the roughness elements in a reach 5.5 m from upstream end of the flume. The average velocity of flow in the vertical centre line was obtained by integrating the above profiles. The mean of the values given by the above profiles was used as the average velocity in the vertical centre line in calculations. The pressure distribution around a representative element was measured as in the case of studies on single element.

4.3 Experimental Procedure (Series of Elements on a Smooth Boundary):

In the studies of roughness placed on smooth boundary, 1 cm high angle iron strips were nailed to the bottom of the flume at the required spacing. Two different spacings, viz 80 cm and 60 cm, yielding $L/h = 80$ and $L/h = 60$ were used. The experiments were performed at two slopes, viz 1/1500 and 1/750.

After the required roughness pattern was placed on the bottom of the flume set to the desired slope, uniform flow was established at a predetermined depth. For each value of L/h , three different depths, viz 5 cm, 10 cm and 15 cm were

used for each slope. The discharge and the water temperature were also noted.

For all the runs the velocity profile was measured over the element as well as midway between the two elements at the centre line of width. Skin friction measurements were made at three sections distant 5 cm, 15 cm and 23.60 cm respectively from one side of the flume using a Preston tube of dia 0.2056 cm. The observations were taken at these three sections over the entire length between two roughness elements. Only the positive shear values were measured. It may be mentioned that the velocity and shear measurements were made beyond a distance of 5.5 m from flume entrance to avoid the effect of entrance disturbances.

From the Preston tube readings, the shear was calculated using the curve given by Patel (13). The equation given by Patel (13) are listed below for reference.

For range, $3.5 < Y^* < 5.3$

$$X^* = Y^* + 2 \log_{10} (1.95 Y^* + 4.10) \quad (4.1)$$

where,
$$X^* = \log_{10} \left(\frac{\Delta^2 \rho d^3}{4\rho V^2} \right) \quad (4.2)$$

and

$$Y^* = \log_{10} \left(\frac{\tau^2 d^3}{4\rho V^2} \right) \quad (4.3)$$

where, T'_0 is skin friction

and d' is the diameter of the Preston Tube

and Δp_p is Preston Tube reading

In range, $1.5 < Y^* < 3.5$

$$Y^* = 0.8287 - 0.1381 X^{*2} + 0.1437 X^{*3} - 0.006 X^{*4} \quad (4.4)$$

Finally in Range, $Y^* < 1.5$

$$Y^* = 0.5 X^* + 0.037 \quad (4.5)$$

CHAPTER - 5

ANALYSIS OF EXPERIMENTAL DATA

5.1 Preliminary Remarks:

The experimental data collected on the various aspects of the problem have been analysed in this Chapter. The analysis has been carried out on the basis of the functional relationship developed in Chapter III. Firstly the resistance of a single element placed on the boundary has been studied. The data on strip roughness placed on a gravel bed have been analysed later. Lastly the strip roughness data for case of a smooth boundary have been analysed to extend the results of Rangaraju and Gardo (19).

5.2 Resistance of a Single Element:

5.2.1 Pressure Distribution:

The data concerning pressure distribution around the element placed on the bed, have been analysed first. The pressure measurements for any run indicated a reasonably constant value of pressure on the down stream face. Hence, for the sake of convenience the pressure distribution has been shown in a pressure difference form (vide Fig.5.1). Here p_u is the pressure on the upstream face, p_d is the pressure on the downstream face and y is the height measured from the bottom of the flume.

It has been pointed out earlier (15) that such a form

of plotting does reflect all the characteristics of variations of upstream pressure. Fig. (5.1) shows that the pressure on the upstream face is also more or less constant over the height, except for a small height near the top. The variation of p_u along the height for large D/h values can be seen to be smaller than that for small D/h values.

5.2.2 Variation of Drag Coefficient with D/h :

The drag coefficient, C_D , for each run was obtained by integration of the pressure difference diagrams similar to Fig. 5.1. As shown in Chapter 3, C_D is expected to be a function of D/h and Fr . Figure (5.3) shows the variation of drag coefficient with D/h . It is seen that drag coefficient decreases continually with increase in D/h , the decrease being pronounced in the range of D/h between 2.0 and 4.0.

The values of V/\sqrt{gD} are marked opposite to each point on Figure (5.3) and Fr does not seem to have any effect on C_D . However the range of Fr covered in this study is very small and more data are required to ascertain the influence of Fr on C_D .

The curve proposed by Adachi on a 6.4 mm thick strip of height 5 mm placed on the bed of the flume is also plotted in the Figure (5.3). It can be seen that at low values of D/h Adachi's curve agrees with that proposed in this study for strips of zero thickness; at high values of D/h Adachi's curve falls above the one proposed here. It is not known whether

Adachi has used the average velocity in the vertical center line as indeed it should be with the center line pressure measurements. Obviously if the average velocity over the cross-section is used along with center line pressure measurements the computed C_D would be higher. Further, studies by Vijaya Singh (23) on two-dimensional normal plates with various values of t/h have shown C_D to increase with t/h in the range of 0 to 1. Since t/h was 1.08 for strips used by Adachi, the higher values of C_D obtained by Adachi may not be inexplicable.

The drag coefficient for a plate on the bed of an open channel can be predicted using the C_{D_0} v/s δ/h curve proposed by Rangaraju - Garde (See Figure 2.1) along with the equation for blockage, namely

$$C_D = C_{D_0} (1 - h/D)^{-2.85} \quad (2.3)$$

Obviously in fully developed flow in an open channel, $D = \delta$ and hence C_{D_0} can be read from Figure (2.1) for the required value of D/h and then equation (2.3) used to find C_D . Such a procedure has been used to obtain a relation between C_D and D/h . (See Figure 5.3). It is seen that the author's curve falls well above the curve predicted from wind tunnel studies. The difference may be due to the fact that in case of wind tunnel the top boundary was smooth and parallel to flow while in flume water depth decreased just downstream of the element.

This decrease in depth results in higher acceleration of flow which may lead to higher drag coefficient values.

Experimental data have also been plotted in the form $1/\sqrt{C_D}$ v/s $\log D/h$ in Figure (5.2). It is seen that the following relationship fits the data reasonably well:

$$\frac{1}{\sqrt{C_D}} = 0.85 \log_{10} D/h + 0.13 \quad (9.1)$$

5.3 SERIES OF ELEMENTS ON A ROUGH BOUNDARY:

5.3.1 Preliminary Remarks:

It was mentioned earlier that the studies on the rough boundary are performed to test the arguments of Rangoraju-Gardó that for $L/h \leq 40$ the net skin friction is zero and the total resistance of the boundary is equal to form resistance of the roughness elements. If these findings are true then the total resistance of the roughened plate bed (with two-dimensional strips placed on it) should be equal to the total resistance of smooth plane bed with the same arrangement of strips. The data collected on the resistance of the gravel bed with strips placed on it has been analysed in this section to check these premises.

5.3.2 Pressure Distribution:

The pressures measured on the two faces of the roughness

element placed on the bed of the flume indicated that for a given velocity and depth of flow, the pressure over the downstream face was constant. Advantage was taken of this fact in plotting the pressure distribution diagram, on the Figure 5.4, where pressure distribution is shown in form of pressure difference between upstream and downstream face of the element plotted against y/h . These diagrams indicate that except for a small height near the top the pressure on the upstream face also remains constant over the height of the element. The drag coefficient values for each run were computed by the integration of corresponding pressure distribution diagrams. The C_D values were obtained with respect to center line velocity. It can be noted that the average abscissa on the plotted curves of Fig. 5.4 yields the form drag coefficient for the corresponding run. The nature of variation of form drag coefficient with relevant parameter will be studied in Sec. 5.3.4.

5.3.3 Comparison of Form Resistance with the total Resistance:

From the measured values of the drag coefficient, the values of T_0'' were computed from the following equation:

$$T_0'' = C_D \cdot h/L \cdot \rho \cdot V^3/2 \quad (5.2)$$

The values of T_0'' are plotted against T_0 ($T_0 = \gamma R_b S$), for all the twelve runs carried out using strips on a gravel bed, in Figure (55). The agreement between T_0 and T_0'' is fairly

good except for three runs. It may be mentioned here that C_D values determined in the flume are usually liable to some error. The drag coefficient was determined from center line pressure and velocity measurements and the average velocity in the center line was obtained by integration of velocity profiles taken at two different cross-sections. In case of a rough boundary with large strips placed over it, the readings of the conventional Prandtl tube could be affected by the curvature of the flow, thus introducing some error into the measured velocity. It should be noted that any errors in the velocity will introduce larger errors in the computed value of C_D . As such the agreement or the scatter on figure may not provide adequate basis to prove or disprove the contention that for $L/h \leq 40$, the total resistance would be equal to the form resistance of the strips. Comparison of the total resistance in case of smooth and rough boundaries (with the same roughness pattern on them) as done in section 5.3.3.- may be the only logical basis to test the foregoing contention.

5.3.4 Variation of Drag Coefficient:

The dimensional analysis in Chapter 3 has shown that drag coefficient C_D can be expressed as

$$C_D = \phi (D/h, L/h)$$

Rangaraju and Gardo (19) found that for their data the relation between the above parameters can be put in the form

$$\frac{\lambda}{\sqrt{C_D}} = C_1 \log D/h + C_2 \quad (2.8)$$

where, C_1 and C_2 are functions of L/h .

Accordingly in this case also the drag coefficient values computed from measurements on rough boundary are plotted on $\frac{\lambda}{\sqrt{C_D}}$ vs. $\log_{10} D/h$ plots for both the spacings (See Fig.5.6)

The values of C_D determined indirectly (i.e. by taking total resistance equal to form resistance) for the smooth boundary data of Rangaraju-Garde are also plotted on this figure. While a majority of the rough boundary data show agreement with the data for smooth boundary, some points indicate a lower value of C_D than for the smooth boundary at corresponding D/h values. The probable reasons for this scatter have been discussed previously. From Fig.(5.6) one may conclude that the drag coefficient of the strip (for a given arrangement) is not significantly affected by the roughness of the plane boundary.

5.3.3 Analysis of Total Resistance

It has been shown in Chapter 3, that the total resistance of the rough boundary can be expressed by the Equation 3.9 i.e.

$$\frac{V}{V_*} = \phi (R_b/h, L/h)$$

Accordingly the data on rough boundary for the two different L/h values are plotted on a graph of V/V_* vs $\log_{10} R_b/h$ (See Fig.5.7).

The data of Rangaraju and Garde on a smooth boundary for these two spacings are also plotted on Figure 5.7. It is interesting to note that data for rough boundary show good agreement with the data obtained from experiments on smooth boundary for both the spacings. Since the skin friction would be otherwise significant in case of the rough boundary the agreement of rough boundary data with those of the smooth boundary may be taken to substantiate the premise of Rangaraju and Garde that the net skin friction is zero for $L/h \leq 40$.

For strips spaced at $L \leq 40 h$, analysis has been carried out on the assumption that the net friction over a distance of $35 h$ downstream of the element is zero. The distance $35 h$ was used on the basis of Plate's results.

5.3.6 Analysis of Velocity Profiles:

Typical velocity profiles for both $L/h = 20$ and 40 are shown in dimensionless form in Fig. 5.8 and 5.9 respectively. The profiles have been shown for two different depths in each case. These profiles were taken at two different sections along the length, as indicated on the figures. The data for both the spacings show a break in the profile and the inapplicability of a single velocity distribution law over the whole depth. The break in velocity profile has been previously reported by Morris(11) Adachi(1), O'Loughlin (12). It has also been reported by some

of these investigators that the velocity distribution over the element differs appreciably from that between elements. But it is interesting to note from Fig. 5.9 that the velocity distribution one quarterway and midway between elements is practically the same for $L/h = 40$. Similarly for $L/h = 20$, velocity profiles tend to coalesce. It is quite likely that the velocity profile over the element may differ from the profiles taken between the roughness elements. But no profile was taken over the element in this series of tests.

A comparison of the velocity profiles has also been made with the velocity profiles for the smooth boundary with roughness elements obtained by Rangaraju (17). The curves on the Figures 5.8 and 5.9 represent the smooth boundary velocity profiles. Three of the four typical profiles presented here show these curves. In case of the fourth (i.e. for $L/h = 40$ and $D = 32.0$ cms) no velocity profile was available for smooth boundary, hence no comparison has been made in this plot. It is seen that velocity profiles for rough boundary and those for smooth boundary are similar which indicates that the frictional resistance of the boundary has no appreciable effect on the velocity distribution in the channel and it remain practically unaltered.

5.4 Series of Elements on a Smooth Boundary:

5.4.1 Preliminary Remarks:

In this section, the data concerning the resistance of two-dimensional strips placed on a smooth boundary have been analysed. Firstly the total resistance of boundary has been studied; this is followed by an analysis of the data concerning skin friction. These results have been used subsequently to determine the relation between form drag of strips and their geometry. Firstly the approach evolved here is used to predict the resistance for Basha's runs (2), and the predicted values are compared with the observed values.

5.4.2 Analysis of Total Resistance:

It was shown in Chapter 3 that the total resistance can be expressed as

$$\frac{\bar{V}}{V_*} = \Phi (R_b/h, L/h)$$

The conventional resistance equation is,

$$\frac{\bar{V}}{V_*} = \frac{2.30}{K} \log_{10} \frac{R_b}{h} + A_1 \quad (5.3)$$

where K is the Karman's constant and A_1 is a constant dependent on the type and arrangement of roughness elements.

The above equation predicts a linear relationship between \bar{V}/V_* and $\log_{10} \frac{R_b}{h}$. On the basis of above equation an effort was made to study the variation of \bar{V}/V_* with $\log_{10} \frac{R_b}{h}$.

Fig.(5.10) shows this plot for the two spacings tested during the study. It shows that a unique relation exists between these parameters for a particular spacing. The equations governing the resistance can be written as

$$\frac{\bar{V}}{V_*} = \frac{2.30}{K} \log_{10} \frac{R_b}{h} + 5.95 \text{ for } L/h = 60 \quad (5.4)$$

$$\text{and, } \frac{\bar{V}}{V_*} = \frac{2.30}{K} \log_{10} \frac{R_b}{h} + 6.90 \text{ for } L/h = 80 \quad (5.5)$$

This indicates that $K = 0.396$ for this type of roughness and the resistance for $L/h = 80$ is greater than for $L/h = 60$.

5.4.3 Variation and Local Skin Friction Coefficient:

The local skin friction coefficient C_f could be defined as

$$C_f = \frac{\tau'_0}{\rho \bar{V}^2 / 2} \quad (5.6)$$

where τ'_0 is the shear stress at a distance x from the element (see Fig. 3.1). As mentioned earlier, the skin friction measurements were made along three rows parallel to the flow - at a distance of 5 cm, 15 cm and 23.6 cm from the side wall. It was noticed that, in general, the shear stress (at any distance x from the element) close to the wall tended to be about higher than that on the centre line. However, one would expect the shear on the centre line to be highest. Nevertheless the average value of τ'_0 along the width was used in the

computation of C_f .

Figures (5.11) and (5.12) show the variation of local skin friction coefficient C_f with x/L , x/h and \bar{V}_x/ν . Data for both $L/h = 80$ and 60 have been plotted on these figures. All the figures indicate a similar trend - i.e. C_f values increase with of the above parameters. However there is no unique relation between C_f and any of these parameters. No third parameter, which would systematise the scatter on these figures, could be found.

The local friction coefficient for the developing turbulent boundary layer is given by,

$$C_f = \frac{0.059}{R_x^{1/5}} \quad (5.7)$$

This relationship has been plotted in Figure for comparison and shows a marked variation from the nature of variation obtained in the present investigation. In case of normal turbulent boundary layer C_f values decrease with increase of Reynold's number whereas in the present study a completely different trend is indicated. This may be because of the fact that the boundary layer downstream of the standing eddy is a redeveloping boundary layer.

5.4.4 Variation of Average Skin Friction Coefficient:

It was shown in Chapter 3 that for computing average skin friction coefficient two approaches are possible. In the I approach the shear in the standing eddy is assumed to be

zero while in II approach it is assumed that the net skin friction for a length of 3δ from the element is zero. Obviously the friction coefficient values obtained from these two approaches would be different. The variation of these friction coefficient values with the pertinent parameters will be discussed in the following sections.

3.4.3 I Approach (Assuming Zero Shear within Eddy):

Referring to Figure 3.1 (of Chapter 3) the average drag coefficient C_{f_1} was defined as,

$$C_{f_1} = \frac{\text{Area ABC}}{L \rho \frac{V_0^2}{2}} \quad (3.8)$$

$$= \frac{F_0}{L \rho \frac{V_0^2}{2}} \quad (3.9)$$

where F_0 is the total positive skin friction between two roughness elements per unit width.

Another drag coefficient C_{f_2} can be defined as

$$C_{f_2} = \frac{F_0}{L_2 \rho \frac{V_0^2}{2}} \quad (3.10)$$

$$= C_{f_1} \cdot L/L_2 \quad (3.11)$$

The variation of C_{f_1} and C_{f_2} with the relevant parameters may now be studied.

Variation of C_{f_1} and C_{f_2} with $\frac{\bar{V}R_b}{\nu}$:

It is expected that C_{f_1} and C_{f_2} would be functions of Reynolds number. The Reynolds numbers that can be considered significant are $\bar{V}R_b/\nu$ and $\bar{V}L/\nu$. Figures 5.13 and 5.14 show variation of C_{f_1} and C_{f_2} with $\bar{V}R_b/\nu$ respectively. It is seen that C_{f_1} and C_{f_2} decrease with increase in Reynolds number of main flow. In both the figures data for the relative spacings tested viz. $L/h = 60$ and $L/h = 80$, fall together yielding a unique relationship.

The equation of the experimental line in Fig. 5.13 is,

$$C_{f_1} = \frac{0.323}{\left(\frac{\bar{V}R_b}{\nu}\right)^{0.423}} \quad (5.12)$$

Similarly the straight line of the Fig. 5.14 could be given by the equation,

$$C_{f_2} = \frac{0.688}{\left(\frac{\bar{V}R_b}{\nu}\right)^{0.48}} \quad (5.13)$$

Variation of C_{f_1} and C_{f_2} with $\bar{V}L/\nu$:

The plots of C_{f_1} and C_{f_2} against the parameter $\bar{V}L/\nu$ are shown in Fig. (5.15) and (5.16) respectively. These figures indicate that skin friction coefficient decreases with increase of $\bar{V}L/\nu$. Again in both cases experimental points for

different spacings fall in such a way that separate lines could be drawn for each spacing.

5.4.6 II Approach (Considering Skin Friction Beyond 35h):

As pointed out in Chapter 3, the net skin friction of the plane boundary could be supposed to be the skin friction beyond a distance equal to 35h from the element, on the basis of Plate's results (13). Accordingly net skin friction would be effective over the area BCDE (See Fig.3.1). Hence C_{f_3} could be defined as

$$C_{f_3} = \frac{\text{Area BCDE}}{L \rho V^2/2} \quad (5.14)$$

$$= \frac{F_s'}{L \rho V^2/2} \quad (5.15)$$

where F_s' is the positive skin friction per unit width between 35h and total length L between two elements, downstream of an element. The variation of C_{f_3} with the pertinent parameters has been studied below.

Figure 5.17 shows a plot of C_{f_3} with VR_b/ν for all the smooth boundary data. It is seen that C_{f_3} decreases with increase in Reynolds number of the main flow. The data for both the series ($L/h = 60$ and $L/h = 80$) fall together. The equation of line fitting the data is

$$C_{f_3} = \frac{(0.256)}{(VR_b/\nu)^{0.435}} \quad (5.16)$$

The Karman - Prandtl equation for a smooth boundary can be written as

$$\frac{1}{\sqrt{f_s}} = 2 \log_{10} R_s \sqrt{f_s} - 0.8 \quad (5.17)$$

This is usually expressed in graphical form - R_s vs f_s to facilitate direct solution. For an open channel Reynolds number can be written as $4\bar{V}R_b/\nu$ and since the average shear stress (of the smooth boundary) can be written as $\frac{f}{4} \cdot \rho \cdot \frac{V^2}{2}$, hence C_{f_3} becomes, equal to $f_s/4$. Accordingly Equation (5.17) has been modified to show the variation of C_{f_3} with $(4\bar{V}R_b/\nu)$ according to Karman - Prandtl equation. This equation predicts higher C_{f_3} values than those obtained from the straight line of the data of the present investigation (See Fig. 5.17). The difference is because of the fact that Karman - Prandtl equation is valid for a boundary where friction remains constant. In the present case frictional resistance of the smooth boundary is constantly varying because of the redeveloping boundary layer.

Fig. 5.18 shows plot of C_{f_3} vs. $\bar{V}L/\nu$. The friction coefficient decreases with increase of $\bar{V}L/\nu$. As in Fig. 5.15 and 5.16 different lines are obtained for the two different values of L/h on which the investigation was carried out. It may be seen that the scatter in case of individual spacings in this plot is much smaller than the scatter in either Fig. 5.15 or 5.16.

5.4.7 Variation of L_1/h vs. \bar{V}_{R_1}/ν :

The length of standing eddy for different roughness patterns used in this study was computed from the shear distribution diagrams. The curves of measured skin friction vs x were extrapolated to find the point at which the skin friction is zero. This was taken as the limit of the standing eddy. The length of the standing eddy has been plotted in a dimensionless form in Fig. 5.19 which is a plot of L_1/h against \bar{V}_{R_1}/ν . The data reveal different curves for the two different roughness patterns viz $L/h = 60$ and $L/h = 80$. It may be seen that the length of standing eddy increases with the increase of \bar{V}_{R_1}/ν in both cases. The resulting curves from the present investigation indicate a similar trend to that obtained by Chang (3) for a single element which incidentally is the limiting case of elements in series. The results of the experimental runs conducted by Chang are also plotted on the Fig.5.19.

A plot was also made between L_1/h and D/h but no relation could be established between these parameters. Hence this plot has been omitted from presentation.

5.4.8. Variation of Form Drag Coefficient of Strips

It was shown in Chapter 3, that the form drag coefficient for the strips could be determined in two ways on the basis of two different assumptions. The first one is to neglect the negative friction within the eddy and ascribe the difference

of total shear and measured positive friction to the resistance of strips. The second approach is to assume the net skin friction to be the measured skin friction values beyond $33h$ from the element and find τ_0'' accordingly. The latter procedure has been used here since the rough boundary studies have lent support to the assumptions involved in the second approach.

As shown earlier on the basis of dimensional analysis, the drag coefficient of a roughness element in series can be written as

$$C_D = \phi (D/h, L/h)$$

The drag coefficient for each run was computed using Equations (3.16), (3.17) and (3.18). Assuming a similarity with the semi-logarithmic relation for friction in pipes, plots of $1/\sqrt{C_D}$ vs. $\log_{10} D/h$ were plotted for different spacings. These are shown in Fig. 5.20 which indicates a linear relationship between $\frac{1}{\sqrt{C_D}}$ and $\log_{10} D/h$ for two different L/h values used in this study. Such a relationship was also found by Rangaraju and Gardo in their studies covering a range of L/h from 2.5 to 40.0. It may be seen that there is a tendency for data of different slopes to fall on different lines. No explanation could be given for this tendency and hence average lines are drawn.

5.4.9 Variation of τ_0''/τ_0 vs L/h :

It was mentioned earlier that the experiments of Rangaraju

and Gardo (17) on a smooth boundary having series of roughness elements showed that the total resistance of the boundary could be taken as equal to form resistance of the roughness elements upto a value of $L/h = 40$. In other words upto $L/h = 40$, the frictional resistance of the boundary may be taken as zero. However for larger spacings skin friction of the plane boundary would be important. Fig. shows the values of τ'_o/τ_o (i.e. the ratio of net skin friction to total shear) plotted against L/h . τ'_o/τ_o has been shown to be zero for $L/h = 40$ on the basis of studies by Rangaraju and Gardo. The author's data shows considerable scatter but the parameter τ'_o/τ_o can distinctly be seen to increase with increase in L/h .

B.4.10 Prediction of Shear For Basha's Data

In order to check the validity of the method developed here, use is made of Basha's (2) data on two-dimensional strips of negligible thickness for a relative spacing of 48. This is done as follows. The total resistance is given by

$$\begin{aligned}\tau_o &= \tau'_o + \tau''_o \\ &= C_{f_3} \cdot L \cdot P \cdot \bar{V}^3/2 + C_D \cdot \frac{h}{L} \cdot \frac{\bar{V}^3}{2} \quad (5.18)\end{aligned}$$

In case of Basha's data for $L/h = 48$, the C_{f_3} values for different runs were computed from the Equation (5.13). The values of C_D were computed from the equation (2.3) using the C_1 and C_2 values for a relative spacing of 48 from Figs. 5.21 and 5.22 respectively.

The total resistance T_0 was then computed from the Equation (5.18). The observed and the computed values of T_0 are compared in Fig. 5.24. The values of slope for each run are marked against the corresponding point on the figure.

In general the computed values are within $\pm 15\%$ of the observed values, though the computed values tend to be smaller for data with larger values of slope. This may be due to the presence of surface waves, the resistance of which has not been taken into account in the present method.

5.4.11 Analysis of Velocity Profiles:

The conventional resistance equation can be written

as

$$\frac{V}{V_*} = \frac{2.30}{K} \log_{10} \frac{D}{K_g} + B_1 \quad (5.19)$$

where B_1 = function of roughness geometry

Since V/V_* is constant for a given value of D/h and L/h ,

hence K_g would also be constant for given values of D, h and

L . Accordingly the velocity distribution law could be

written as

$$U/V_* = \phi (\log_{10} y/h) \quad \text{for given values}$$

of D, h and L . On this basis typical data on the velocity

distribution for flow over roughness elements in series has

been plotted in Figures 5.23 and 5.26. The velocity profiles

taken midway between the elements and those over the element

are plotted together for each value of L/h .

It is distinct that the velocity over the element at any given elevation from the bed is always greater than the velocity between the roughness elements at the corresponding elevation. This may probably be on account of the increase in mean velocity over the element.

The difference in velocity profile over the element and midway between the elements, noticed in Figures 5.25 and 5.26, have been previously pointed out by Adachi (1) and Rangaraju and Gardo (17). It is seen from the Figures 5.25 & 5.26 that the difference between velocity profiles over the roughness element and midway between elements is larger in case of larger spacing. Another point to note is that a break in velocity profile occurs in case of both the spacings used here. This fact has also been pointed out by previous investigators (1,9,10,13).

CHAPTER - 6

CONCLUSIONS AND SUGGESTIONS FOR FURTHER STUDY

The present investigation has thrown additional light on the mechanism of resistance to flow over two-dimensional sharp edged artificial roughness elements in an open channel. The main aspects of the problem investigated were form resistance of roughness elements and skin friction of the plane boundary having regular arrangement of roughness elements in series. As a result of the analysis of the data collected during the present investigations the following conclusions are derived:

1. The drag coefficient of a single normal plate kept on the bed of an open channel decreases continuously with increase of D/h .

2. The equation

$C_D = C_{D_0} (1 - h/D)^{-2.85}$ and the curve of C_{D_0} vs δ/h proposed by Rangaraju and Garde from wind tunnel studies is inadequate for the determination of drag coefficient of a roughness element placed on the bed of an open channel.

3. In case of a plane boundary having roughness elements placed on the boundary in series the total resistance may be taken equal to the form resistance of the strips for $L/h \leq 40$.

4. The total resistance of a plane boundary with roughness

elements having $L/h > 40$ can be determined by adding the form resistance of the strips to the skin friction between $33h$ and L downstream of the element. Equations (2.8) and (3.18) along with figures (5.21) and (5.22) enable calculation of the form resistance while equations (5.16) and (3.17) along with figure (5.17) can be used for the calculation of the above frictional resistance.

Suggestions for Further Study:

It is desirable to continue the study of the problem presented herein in order to get a better understanding of the phenomenon of resistance. In this context the following suggestions can be made for further research on the problem:

1. The present investigations used only sharp edged roughness elements spanning the whole width of the flume. Further studies should be carried out with different types of roughness elements.
2. Studies concerning the skin friction of the boundary as well as the total resistance of the boundary should be made with larger spacings.
3. In case of resistance of single element more studies should be made on effect of Froude's number on drag coefficients.

REFERENCES

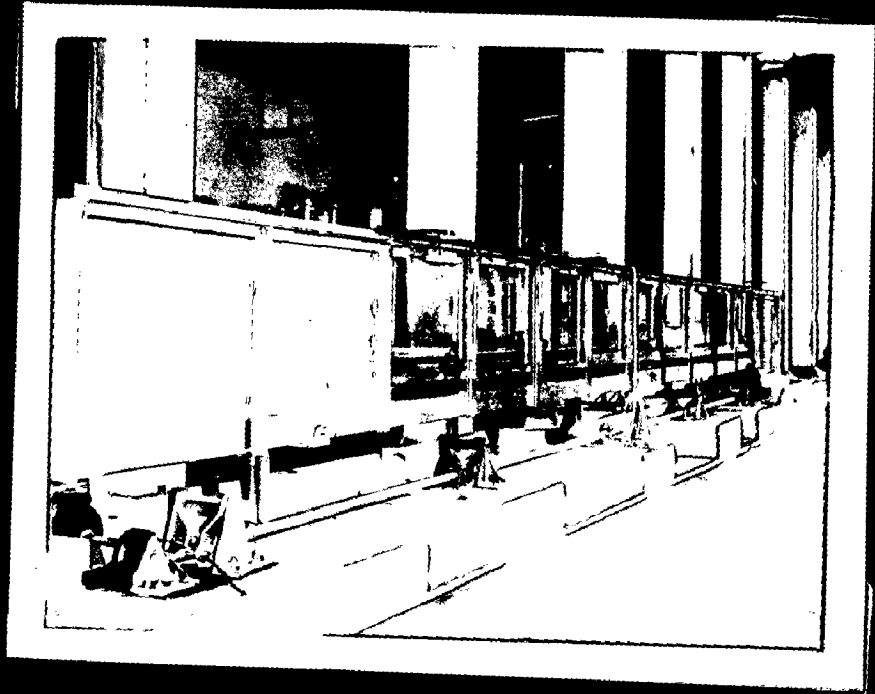
1. Adachi, S., "On the Artificial Strib Roughness" Bulletin No. 69, Disaster Prevention Research Institute, Kyoto University, March 1964, pp 1-20.
2. Basha, M.A., "Resistance Characteristics of Artificially Roughened Open Channels in Relation to those of Alluvial Channels", M.E. Dissertation, University of Roorkee, May 1961.
3. Chang, Fred F.M., "Ripple Concentration and Friction Factor", Journal of Hydraulic Division, ASCE, vol. 96, No. HY 2, Proc. Paper 7067, February, 1970, pp 417-430.
4. Einstein, H.A., and Banks, R.B., "Fluid Resistance of Composite Roughness", Trans. A.G.U., Vol. 31, No.4, August, 1950, pp 603 - 610.
5. Einstein, H.A., and Barbarossa, N.L., "River Channel Roughness" Transactions, A.S.C.E., vol 107, 1942, pp 1121-1146.
6. Good, M.C. and Joubert, P.N. "The Form Drag of Two-Dimensional Bluff Plates Immersed in Turbulent Boundary-Layers", Journal of Fluid Mechanics, vol 31, Part 3, 1968, pp 547 - 582.
7. Herbich, J.B. and Shulits, S., "Large Scale Roughness in Open Channel Flow", Journal of Hydraulic Division, Proc., A.S.C.E., vol 90, November 1964, pp 203 - 210.
8. Johnson, J.W., "Rectangular Artificial Roughness in Open Channels", Trans.A.G.U., vol 25, Part VI, 1944 pp 906-914.

9. Koloseus, H.J., "The Effect of Free-Surface Instability on Channel Resistance", Ph.D. Dissertation, State University of Iowa, August, 1958.
10. Koloseus, H.J., and Davidian J., "Free Surface Instability correlations and Roughness Concentration Effects on Flow over Hydrodynamically Rough surfaces" Geological Survey Water Supply Paper 1592- C.D., U.S. Govt. Printing Office, 1966.
11. Morris, H.M., "Flow in Rough Conduits", Trans. A.S.C.E., vol. 120, 1955, pp 373 - 410.
12. O'Loughlin, E.M. and Macdonald, E.G., "Some Roughness Concentration effects on Boundary Resistance", La Houille Blanche, No.7/1964, pp 773 - 783.
13. Patel, V.C. "Calibration of Preston Tube and Limitations on its use in pressure gradients", Journal of Fluid Mechanics, vol. 23, 1965.
14. Peterson, Dean F. and Mohanty, P.K. "Flume Studies of Flow in Steep Rough Open Channels", Proc., A.S.C.E., vol. 86, November, 1960, pp 55-76.
15. Plate, E.J., "The Drag on a smooth Flat Plate with a Fence immersed in its Turbulent Boundary Layer", Presented at the Fluids Engg. Conference, Philadelphia, A.S.M.E., May, 1964.
16. Powell, R.W., "Flow in a Channel of Definite Roughness", Trans. A.S.C.E., vol. 111, 1946, pp 531-566.

17. Rangaraju, K.G., "Mechanism of Resistance to Flow Over Artificial Roughness Elements", Ph.D. Dissertation, University of Roorkee, Roorkee, May 1967.
18. Rangaraju, K.G. and Garde, R.J., "Resistance of an inclined plate placed on a Plane Boundary in Two-Dimensional Flow", Journal of Basic Engineering, Trans. A.S.M.E., Paper No. 69-FE-3, March, 1970, pp 21-31.
19. Rangaraju, K.G. and Garde, R.J., "Resistance to Flow over Two-Dimensional Strip Roughness", Journal of Hydraulics Division, ASCE, Vol. 96, No. HY3, Proc. paper 7181, March, 1970, pp 815- 834.
20. Roberson, John A. and Chen, C.K., "Flow in Conduits with Low Roughness Concentration", Journal of Hydraulics Division, ASCE, vol. 96, No. HY4, Proc. Paper 7224, April, 1970, pp 941-957.
21. Robinson, A.R. and Albertson, M.L., "Artificial Roughness Standard for Open Channels", Trans. A.G.U., vol 33, No.6, December, 1952, pp 881 - 888.
22. Rouse, H., "Fluid Mechanics for Hydraulic Engineers" Dover Publications, Inc., New York, 1961, p 217, p 228.
23. Rouse, H., Kolosovs, H.J. and Davidian, J., "The Role of Froude number in Open-Channel Resistance", Journal of Hydraulic Research, A.A.H.R., vol. 1, 1963, pp 14-19.
24. Sayre, W.W. and Albertson, M.L., "Roughness spacing in Rigid Open Channels", Trans. ASCE, vol. 128, '63, pp 343-427.
25. Singh, V., "Wind Tunnel Studies of Form Drag on Two-Dimensional Square Normal Plates, M. E. Dissertation, Univ. of Roorkee, Roorkee, Dec. 1969, Fig. 4.5.

26. O' Loughlin, E.M., "Resistance to flow over boundaries with small roughness concentration" Ph.D. Thesis, State University of Iowa, 1965.

FIGURES



Photograph 1 - General View of the Experimental Flume



Photograph 2 - Roughness elements in position on the bottom of the flume glued with gravel.

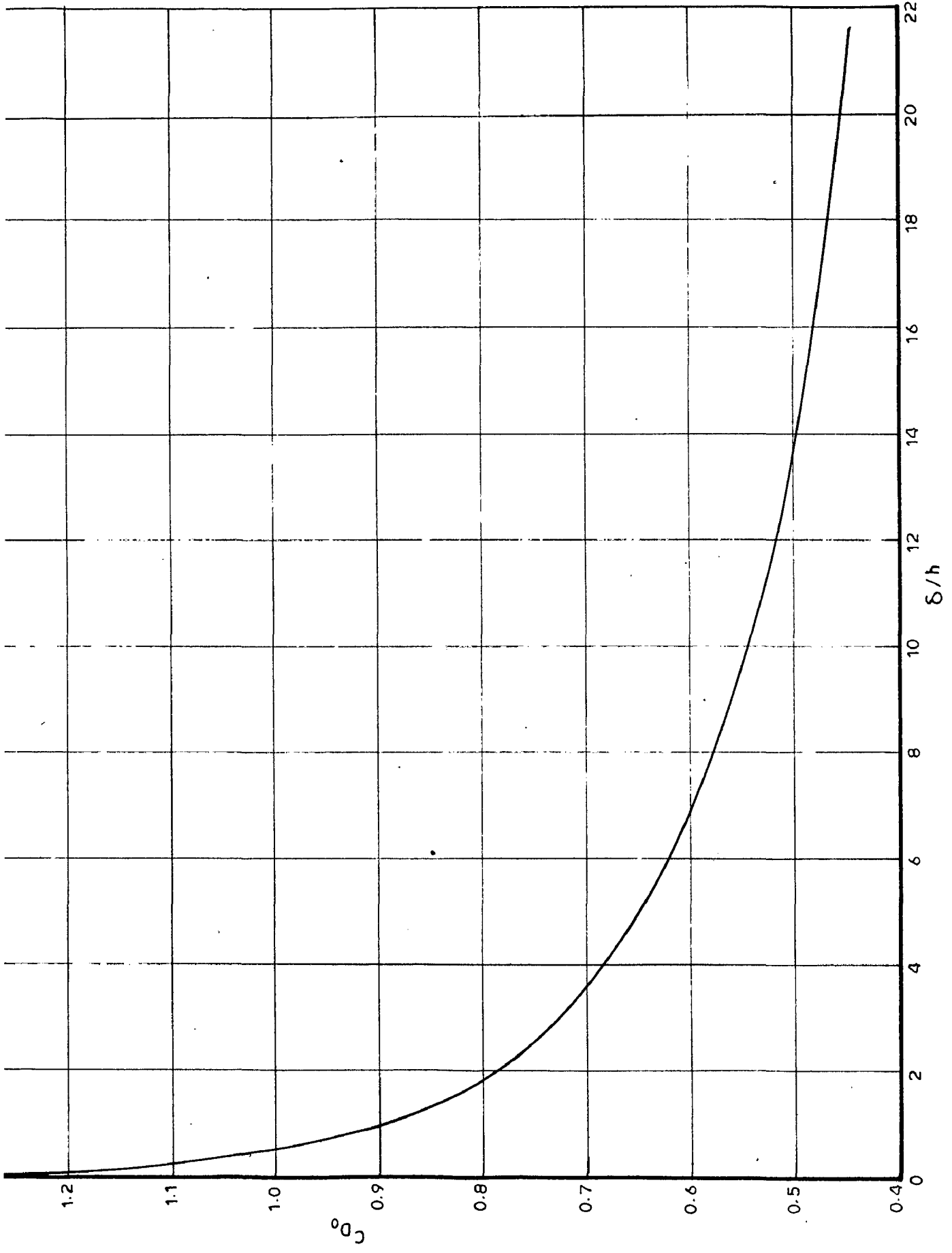


FIG.2.1 - VARIATION OF C_{D_0} WITH δ/h FOR NORMAL PLATES IN BOUNDARY LAYER (REF. 18)

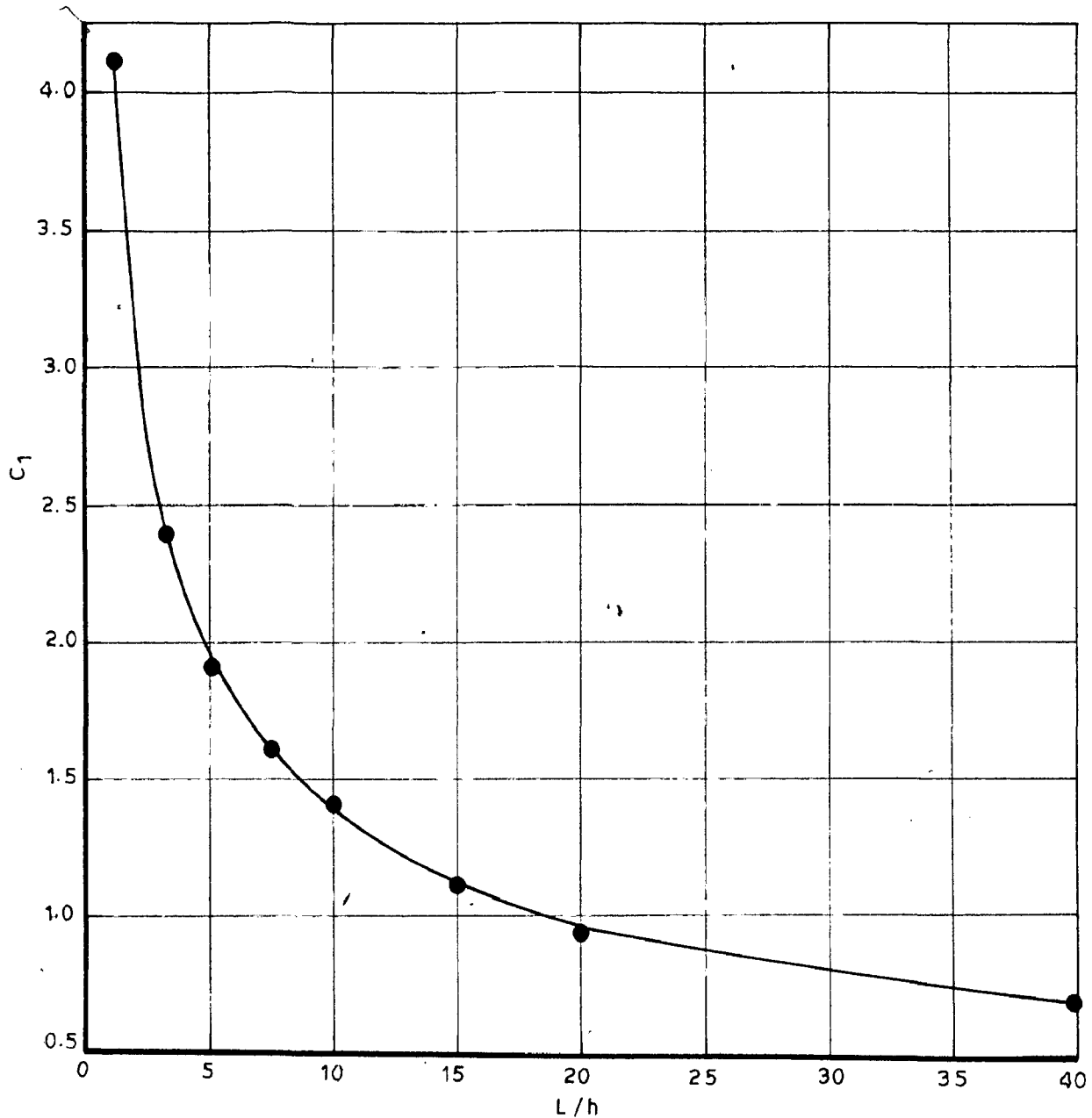


FIG. 2.2 - VARIATION OF C_1 WITH L/h FOR TWO-DIMENSIONAL ELEMENTS IN SERIES (REF. 19)

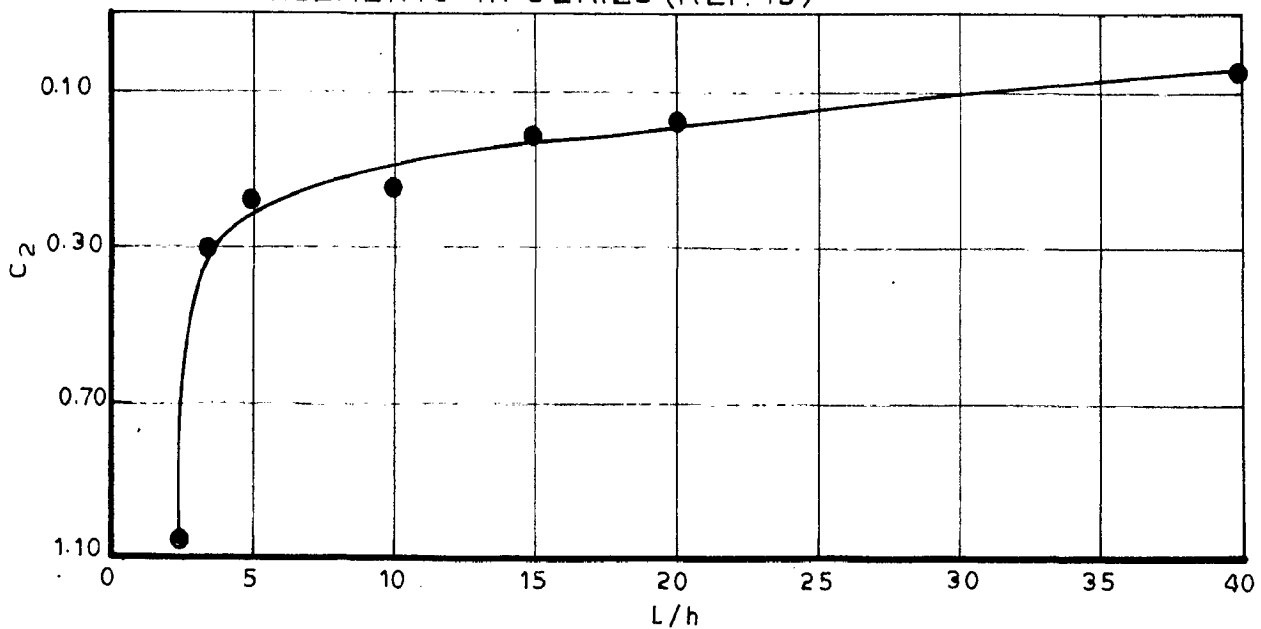


FIG. 2.3 - VARIATION OF C_2 WITH L/h FOR TWO DIMENSIONAL ELEMENTS IN SERIES (REF. 19)

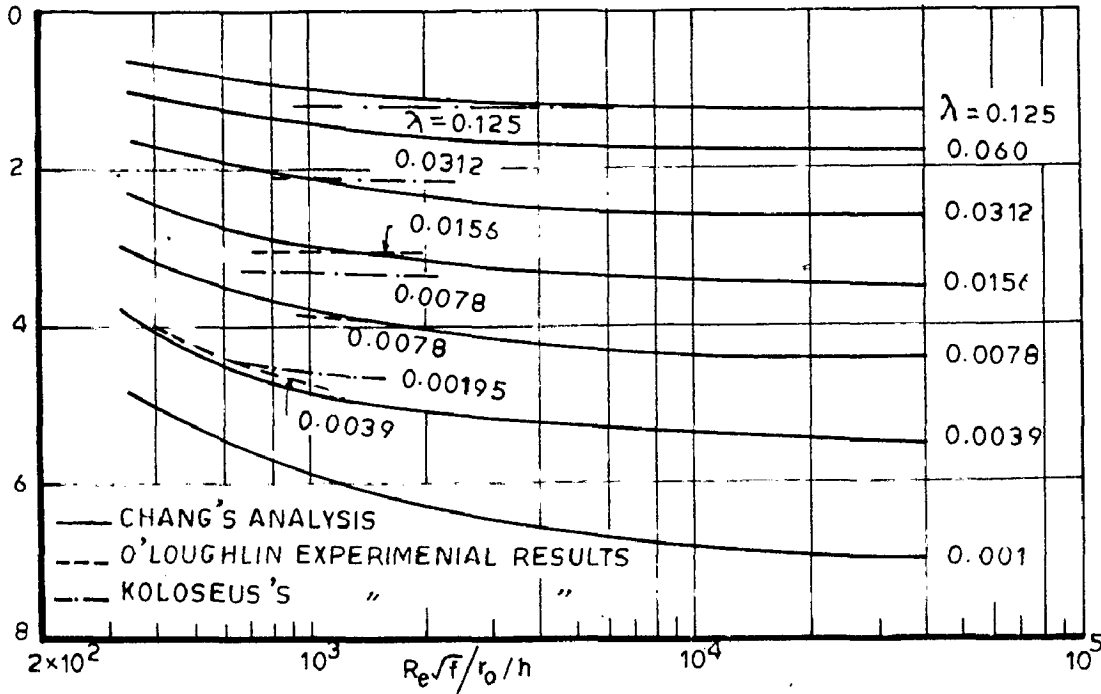


FIG. 2.4 TRANSITION FUNCTIONS FOR CONDUIT ROUGHENED WITH CUBES (REF. 3)

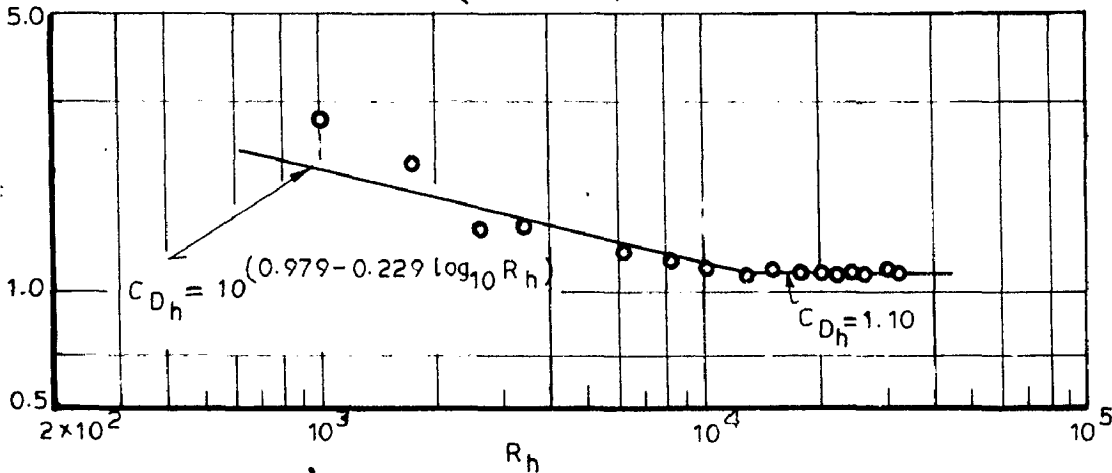
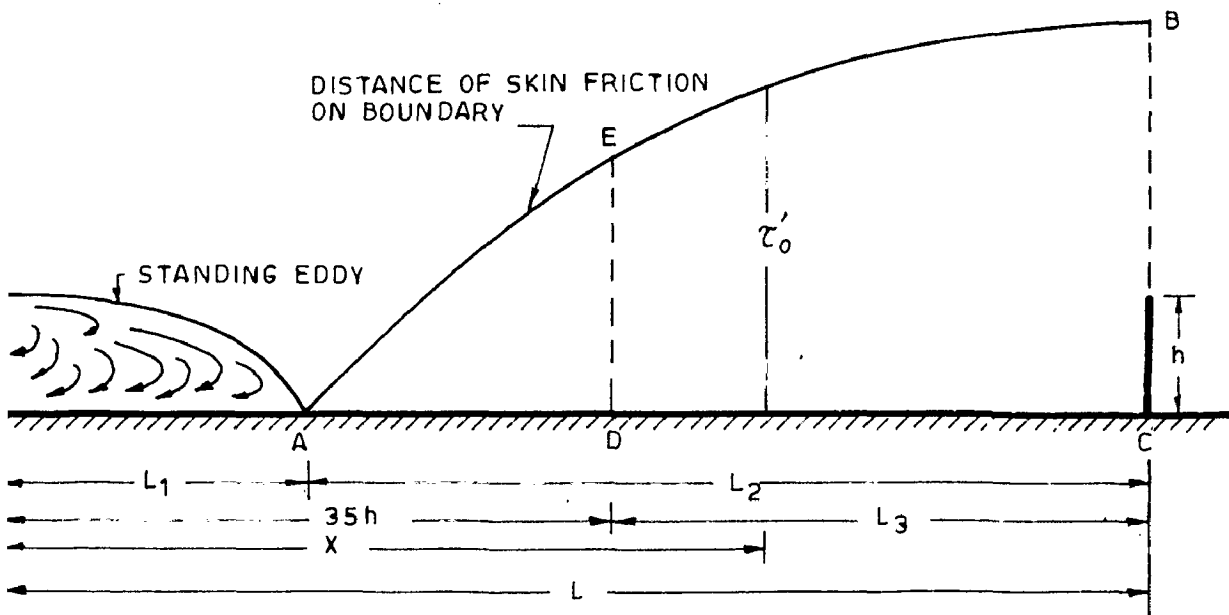
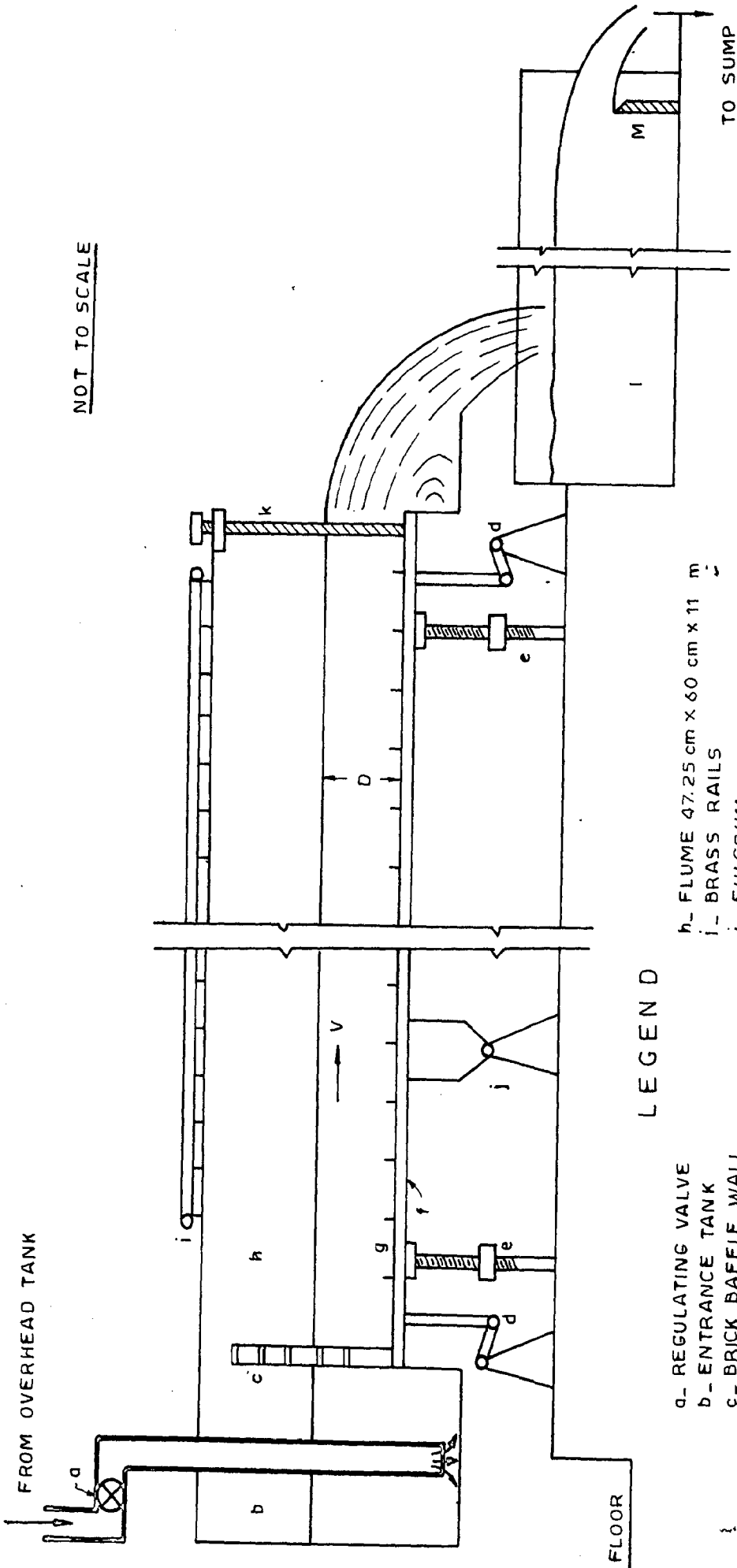


FIG. 2.5 PLOT OF COEFFICIENT OF DRAG VS REYNOLDS NUMBER FOR CUBE (REF. 3)



3.3.1 SCHEMATIC DIAGRAM OF SHEAR STRESS DISTRIBUTION



NOT TO SCALE

LEGEND

- a- REGULATING VALVE
- b- ENTRANCE TANK
- c- BRICK BAFFLE WALL
- d- JACKS
- e- LOCKING ARRANGEMENT
- f- WOODEN FALSE BOTTOM
- g- ROUGHNESS STRIP
- h- FLUME 47.25 cm x 60 cm x 11 m
- i- BRASS RAILS
- j- FULCRUM
- k- TAIL GATE
- l- TANK
- m- RECTANGULAR SHARP-CRESTED WEIR

106734
 LIBRARY UNIVERSITY OF ROOKEE
 ROOKEE.

FIG.4.1 - SCHEMATIC DIAGRAM OF EXPERIMENTAL FLUME

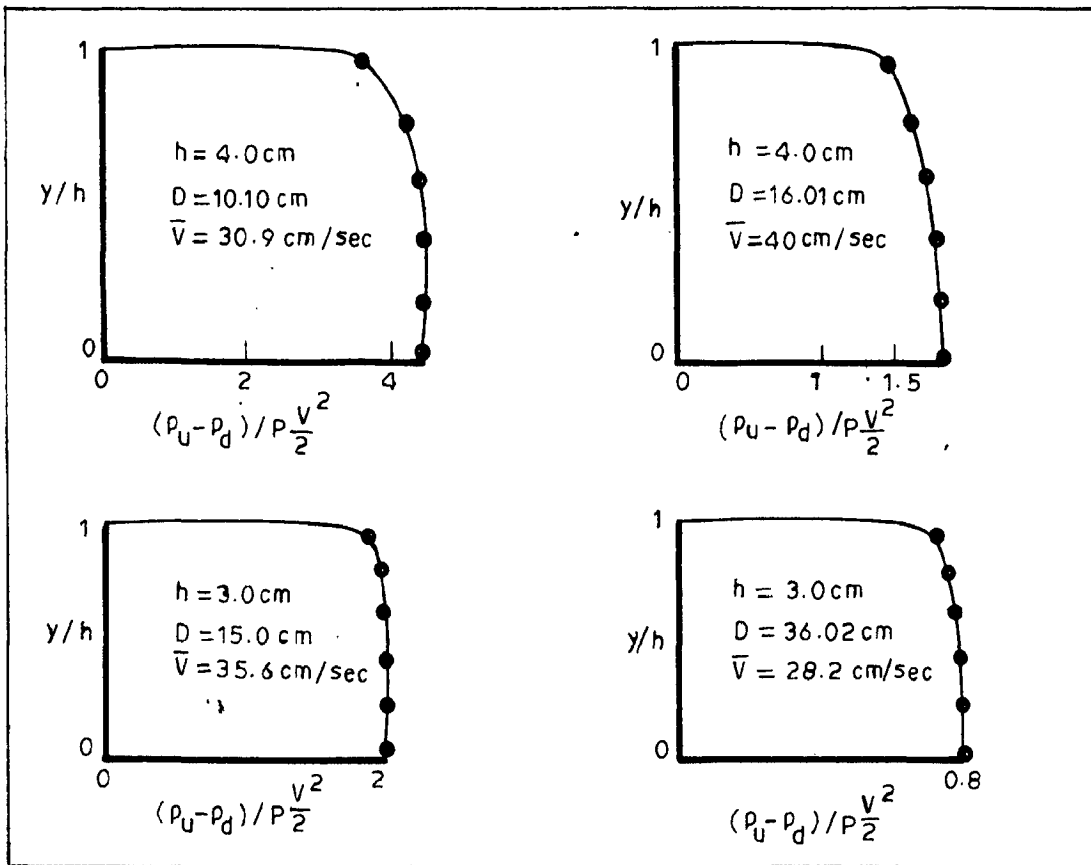


FIG.5.1 _ PLOT OF PRESSURE DIFFERENCE AROUND SINGLE ELEMENT

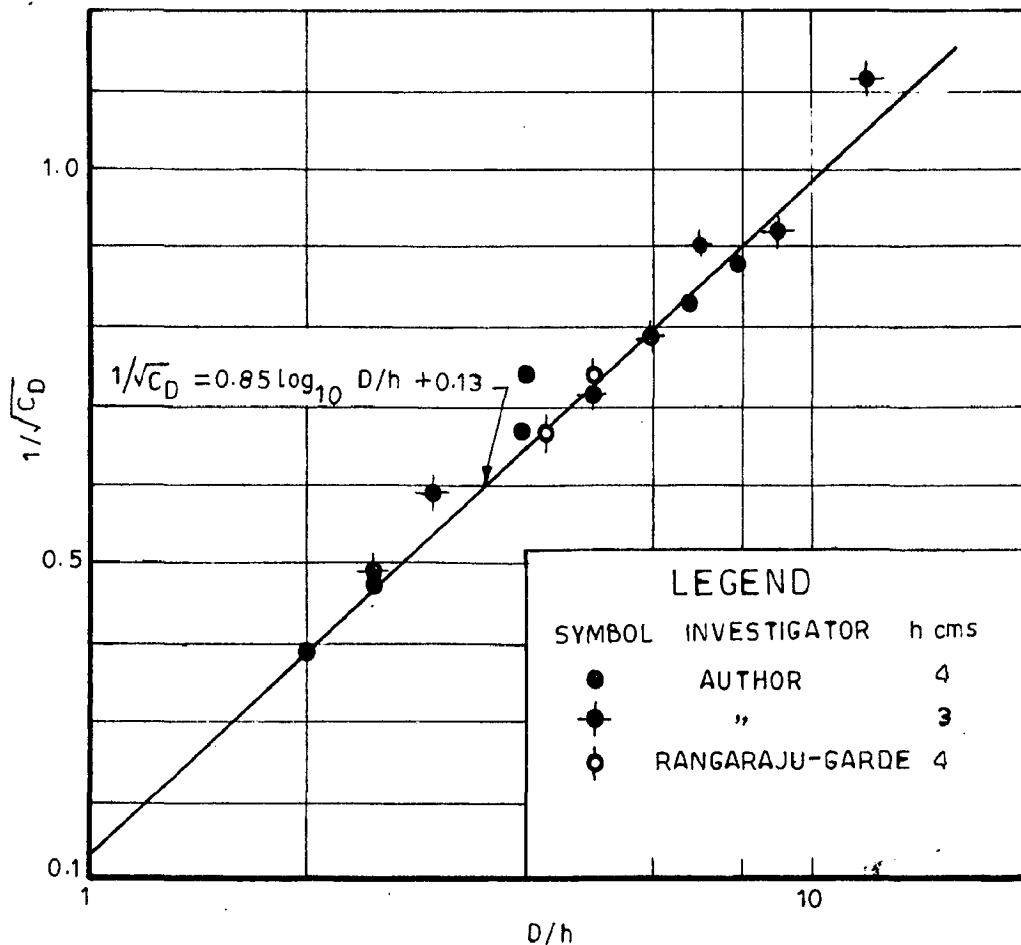


FIG.5.2 _ VARIATION OF $1/\sqrt{C_D}$ WITH D/h FOR SINGLE ELEMENT

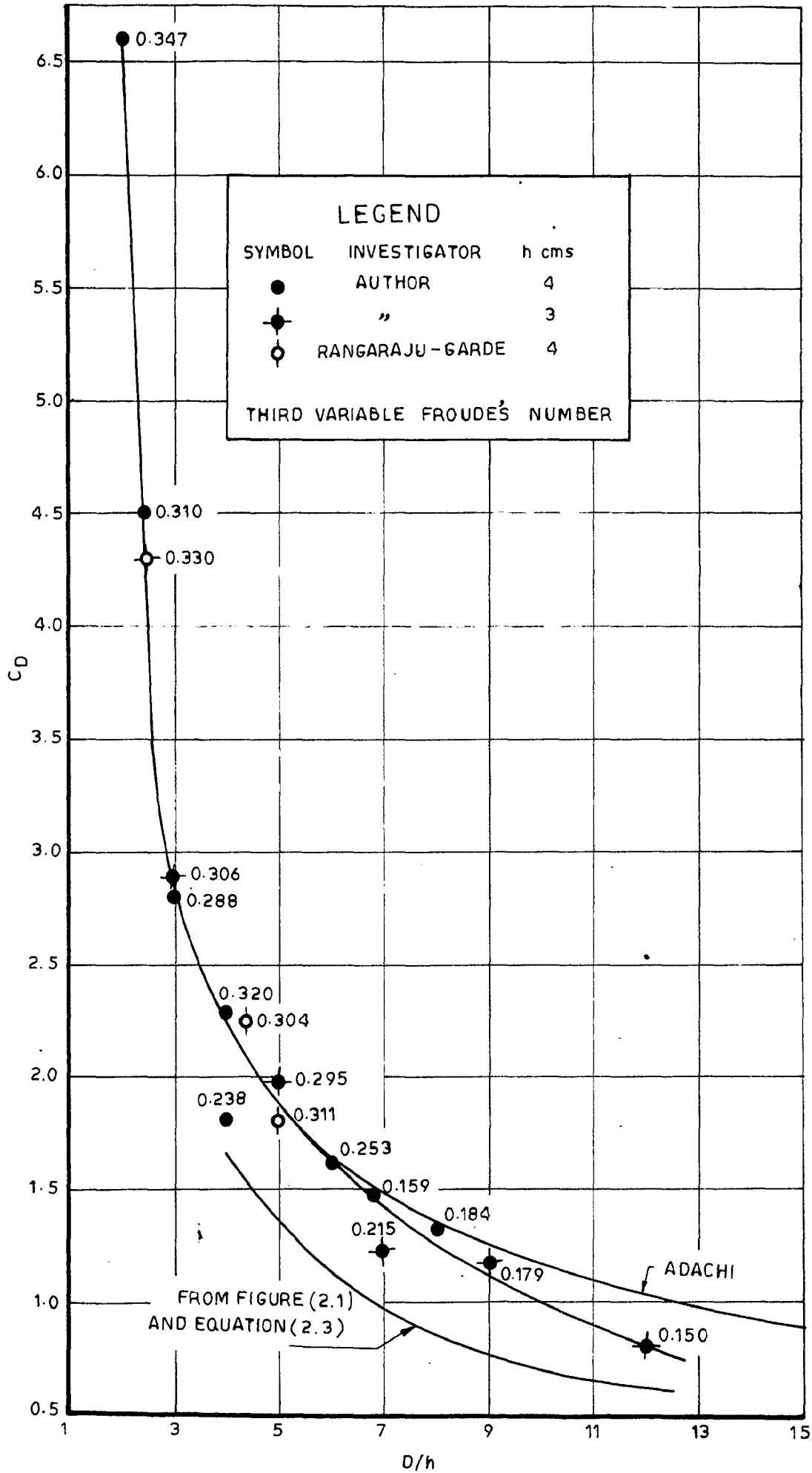


FIG.5.3 - VARIATION OF C_D WITH D/h FOR SINGLE ELEMENT

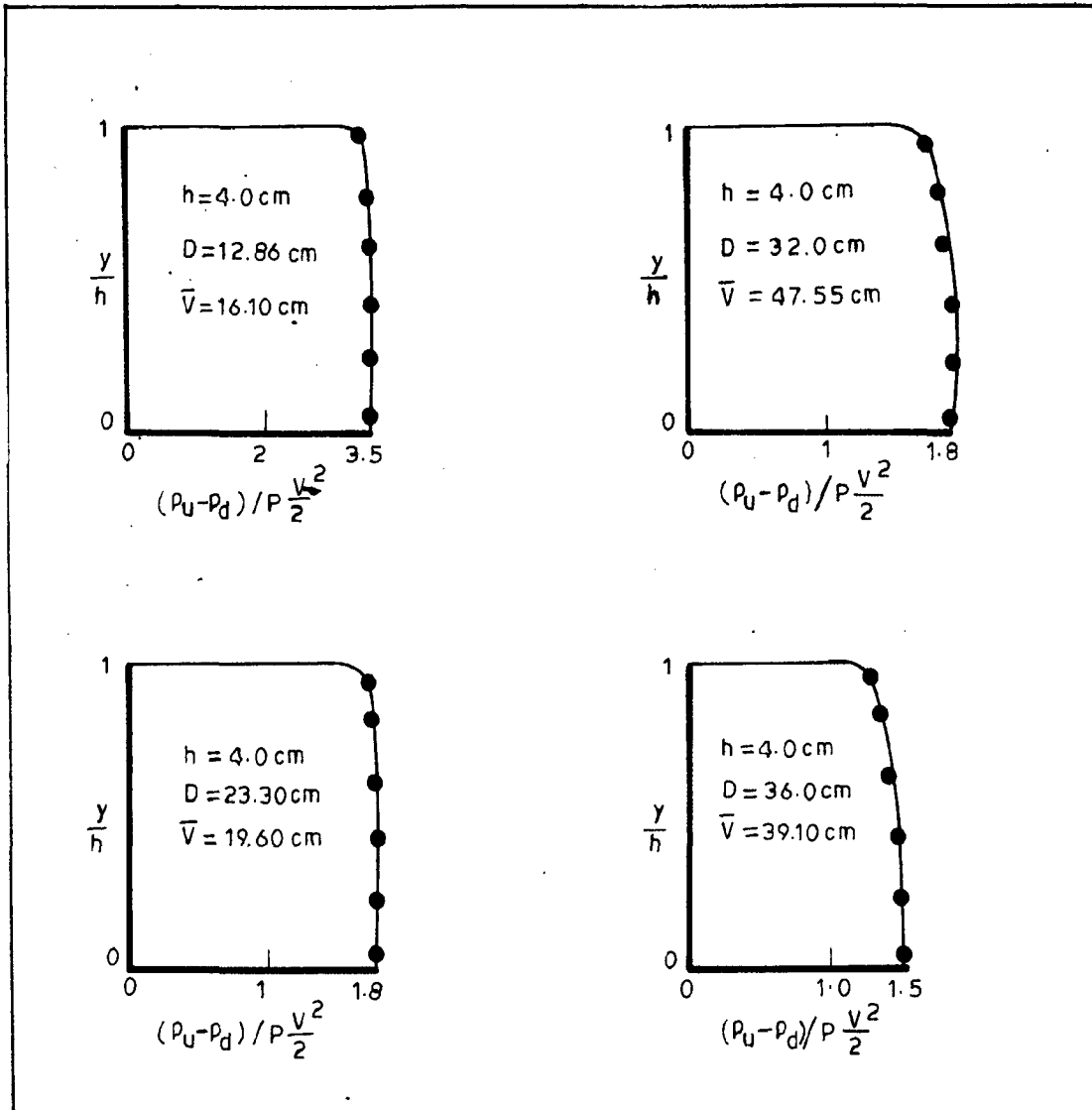


FIG.5.4 - PLOT OF PRESSURE DIFFERENCE AROUND ELEMENTS IN ROUGH BOUNDARY

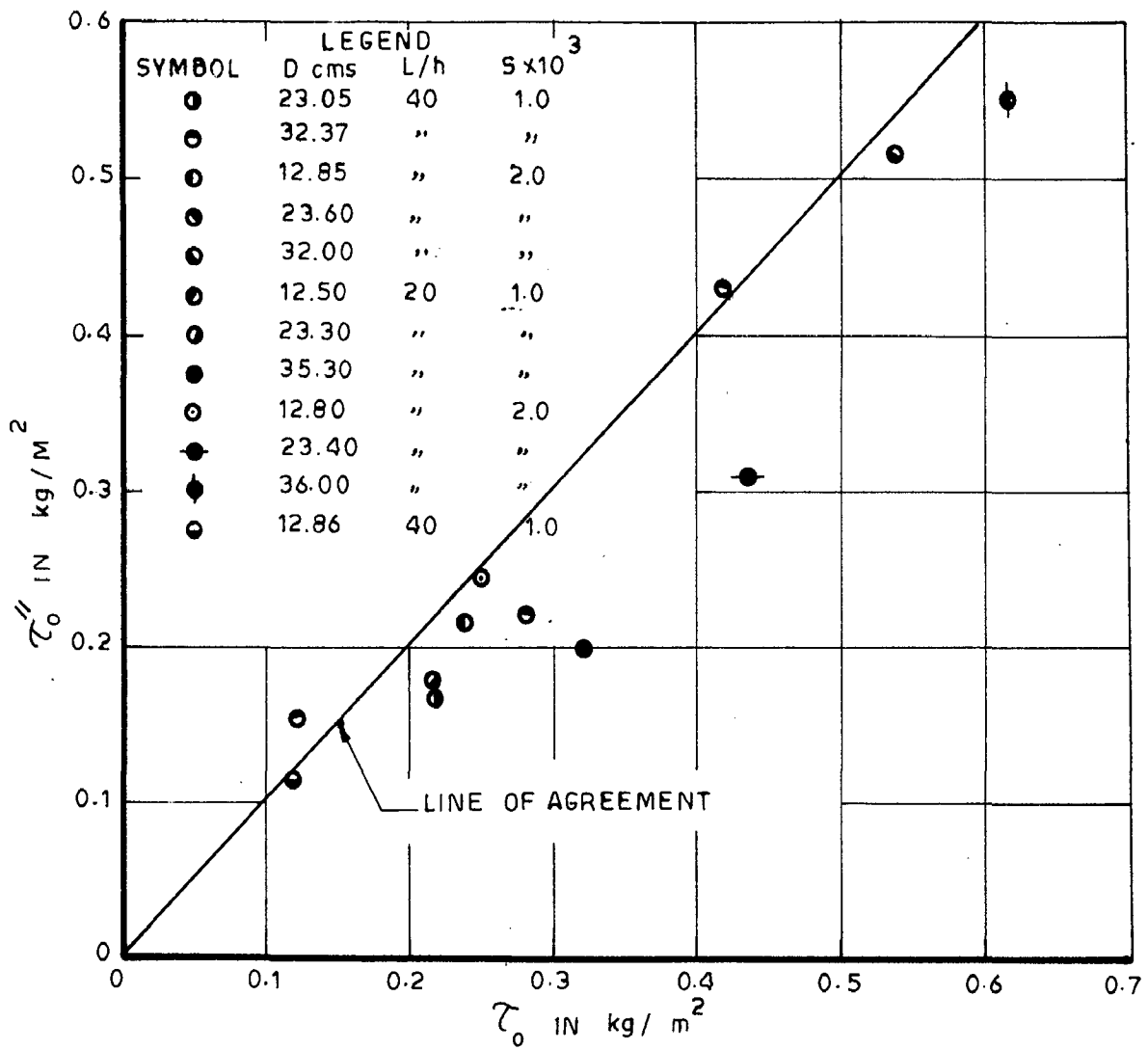


FIG.5.5 - COMPARISON BETWEEN τ_0 AND τ_0'' FOR ROUGH BOUNDARY WITH STRIPS

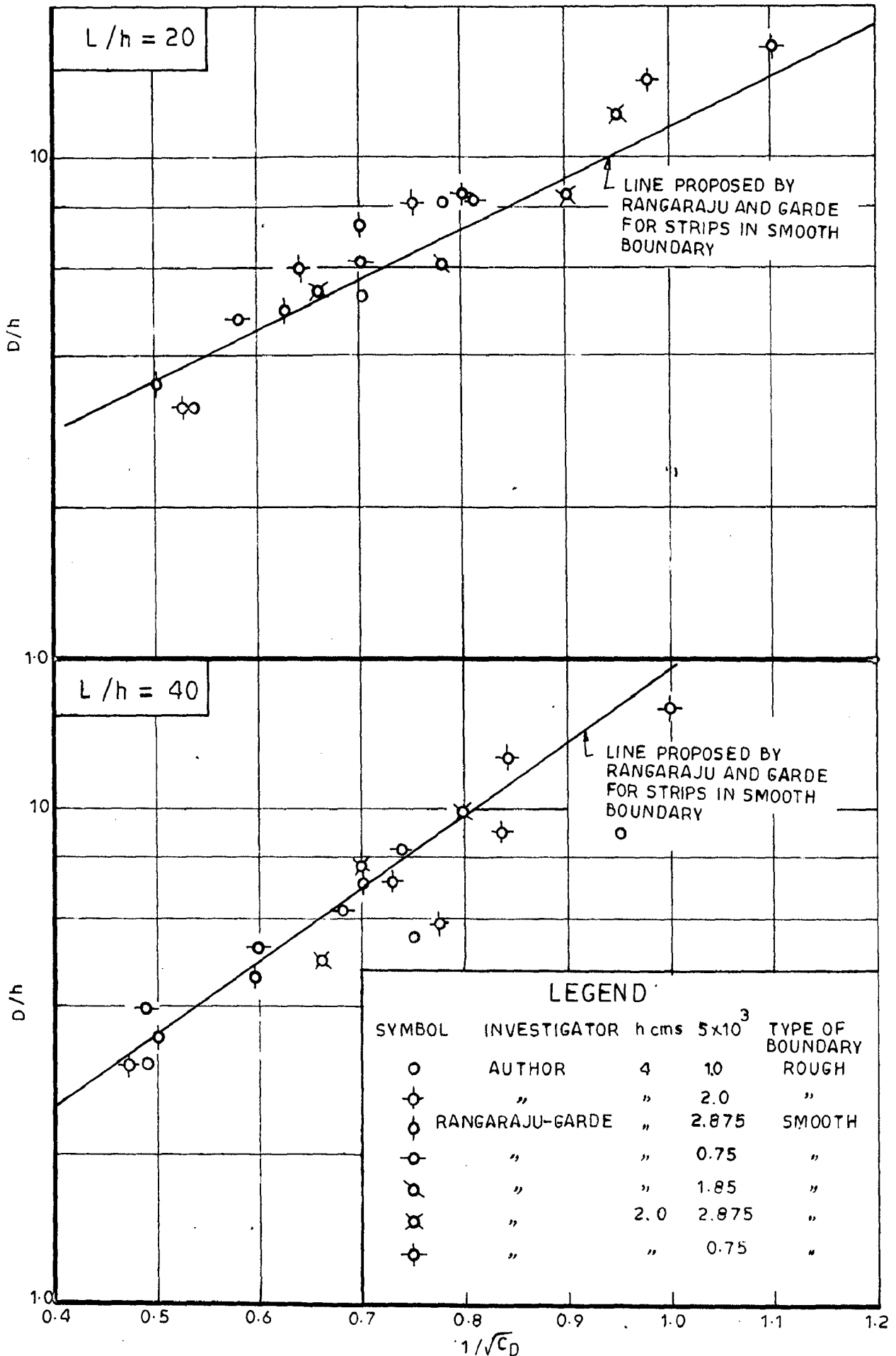


FIG. 5.6-VARIATION OF $1/\sqrt{C_D}$ WITH D/h AND L/h FOR ELEMENTS IN SERIES

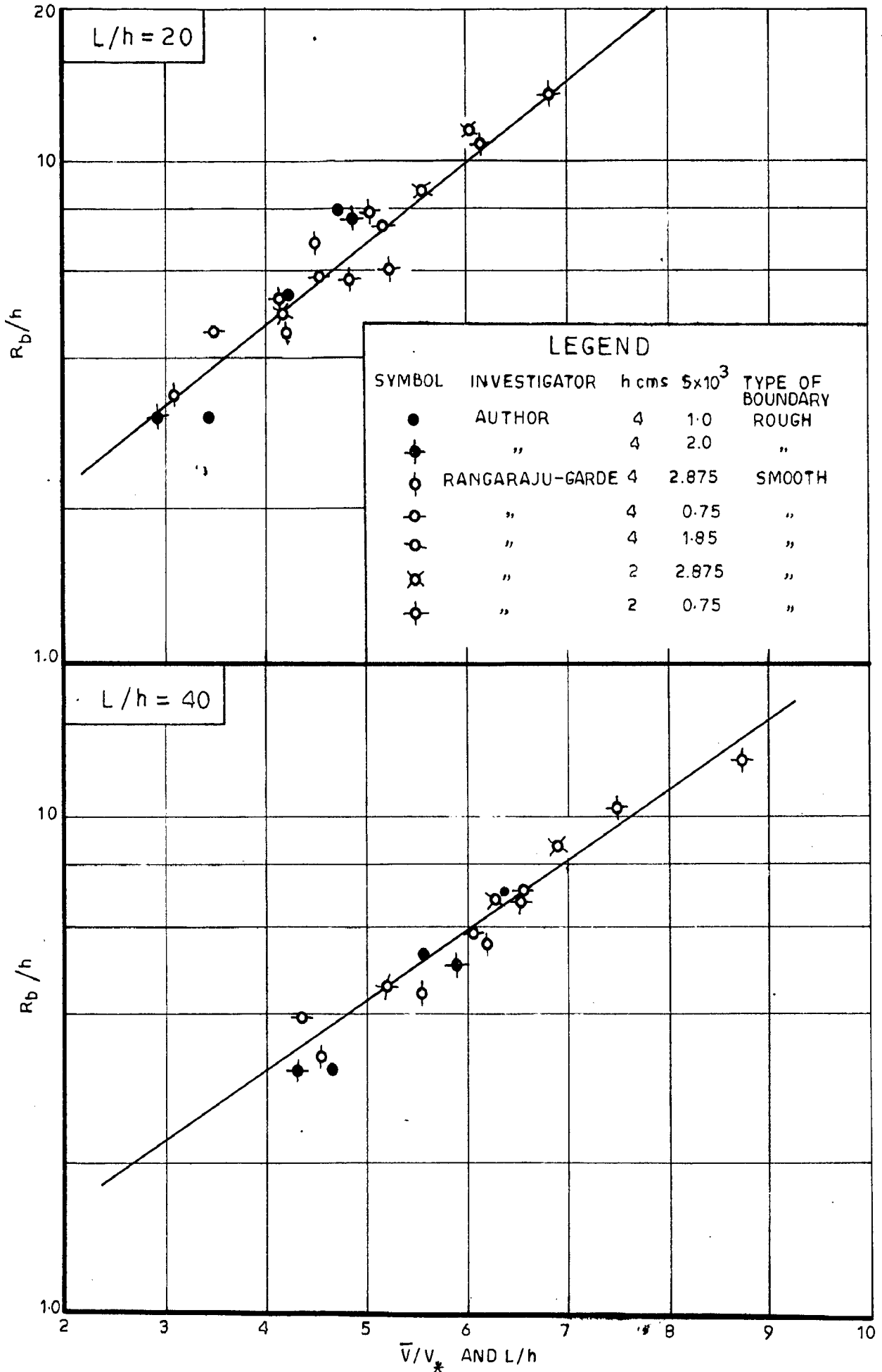


FIG. 5.7 VARIATION OF \bar{V}/V_* VS R_b/h AND L/h FOR ELEMENTS IN SERIES

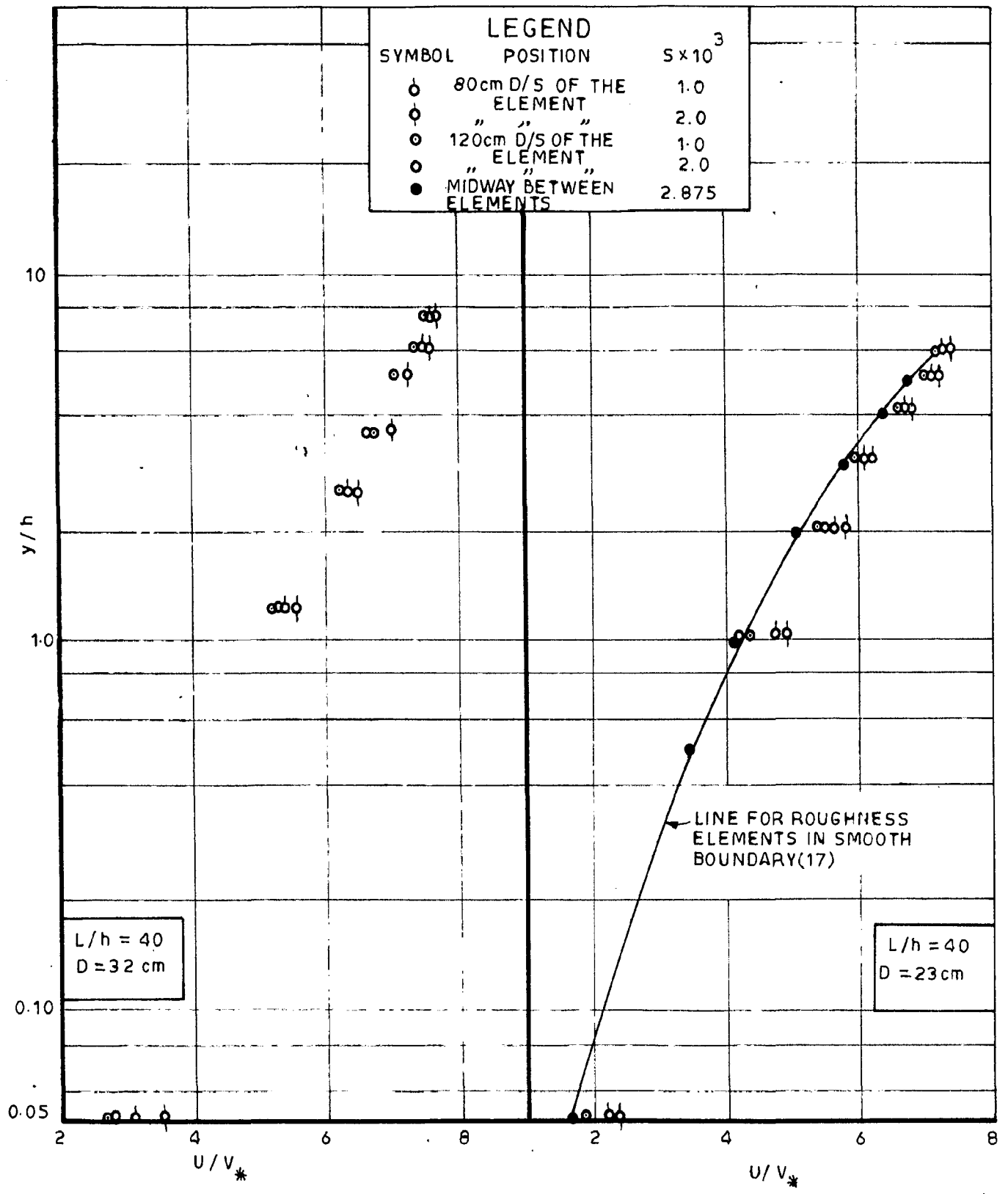


FIG.5.9_PLOT OF U/V_* VS $\log_{10} y/h$ FOR ELEMENTS IN ROUGH BOUNDARY

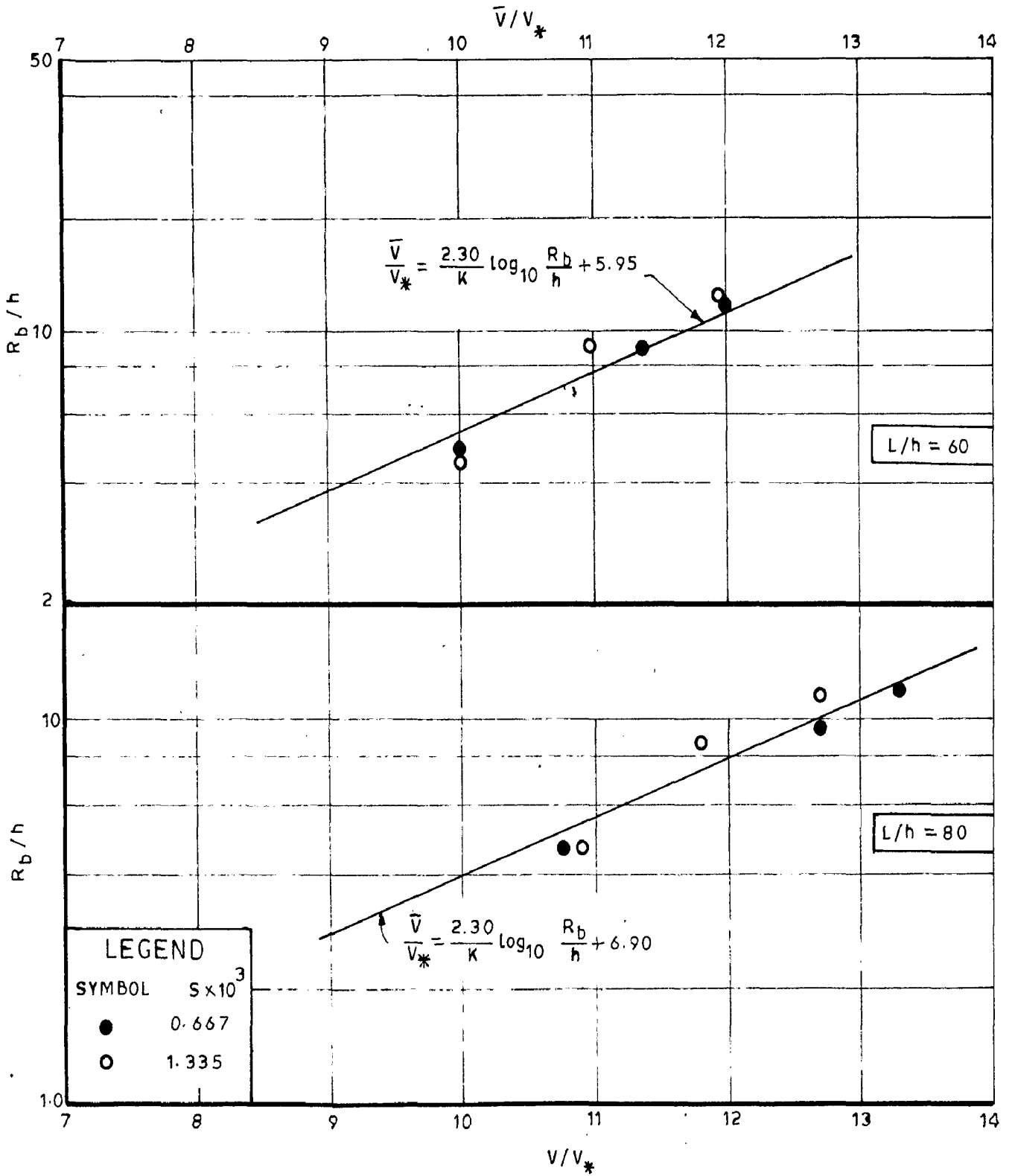


FIG. 5.10 VARIATION OF \bar{V}/V_* WITH R_b/h AND L/h FOR SMOOTH BOUNDAR

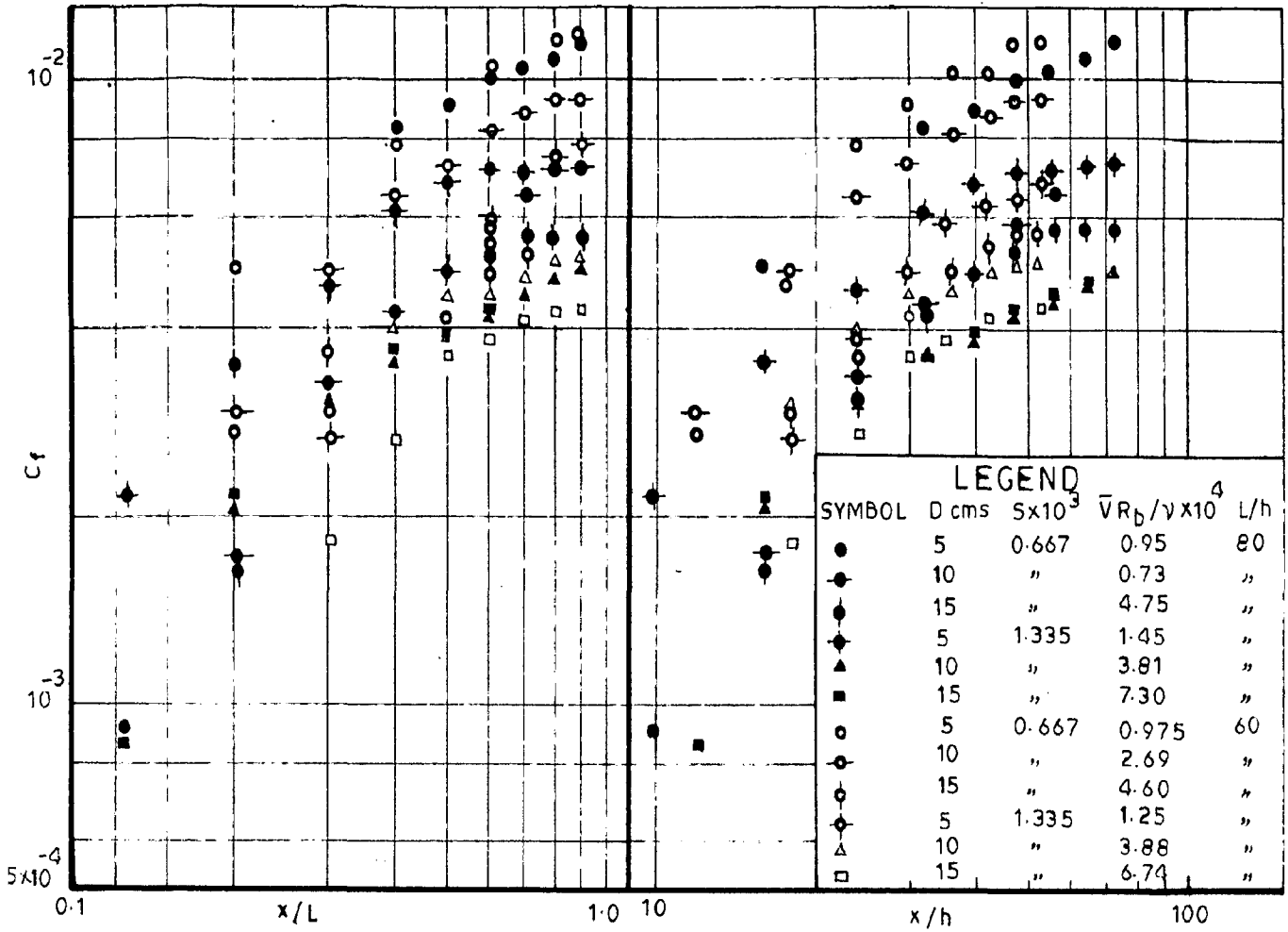


FIG. 5.11 - VARIATION OF C_f WITH x/L AND x/h FOR ELEMENTS ON SMOOTH BOUNDARY

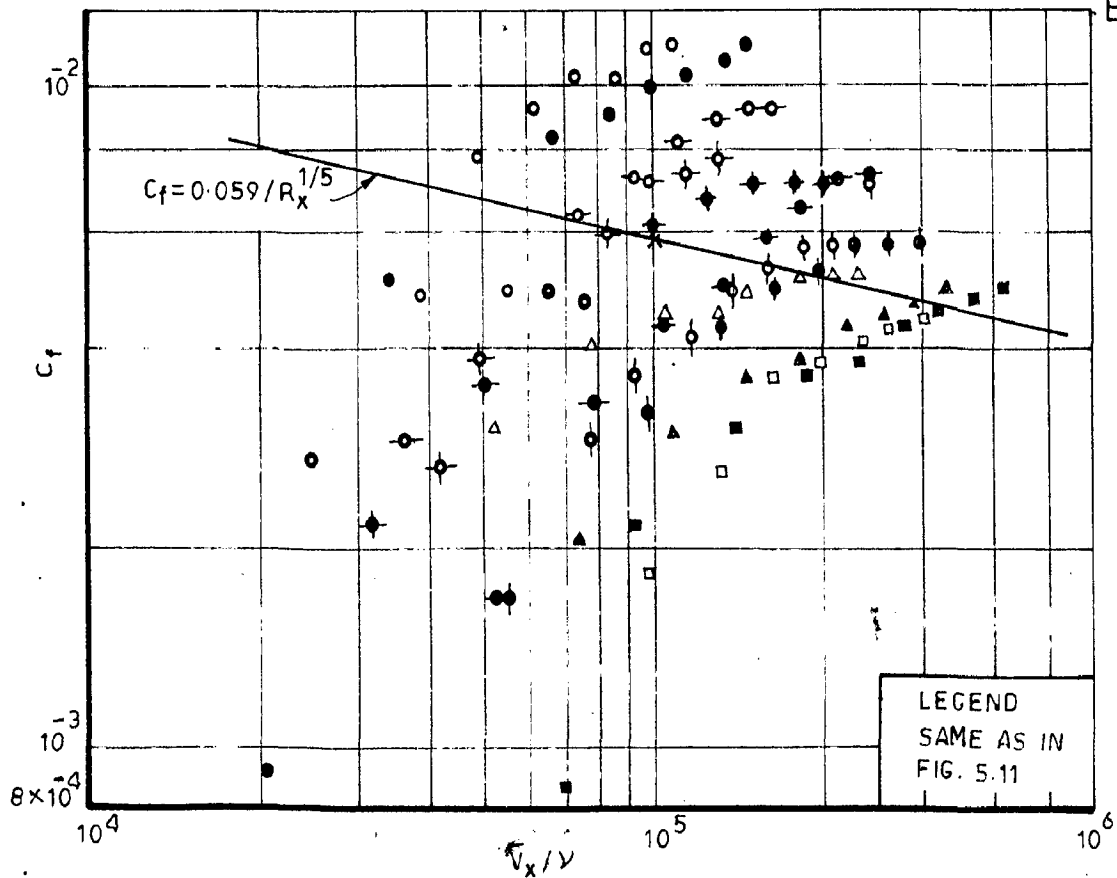


FIG. 5.12 - PLOT OF C_f VS $\bar{V}x/\nu$ FOR ELEMENTS ON SMOOTH BOUNDARY

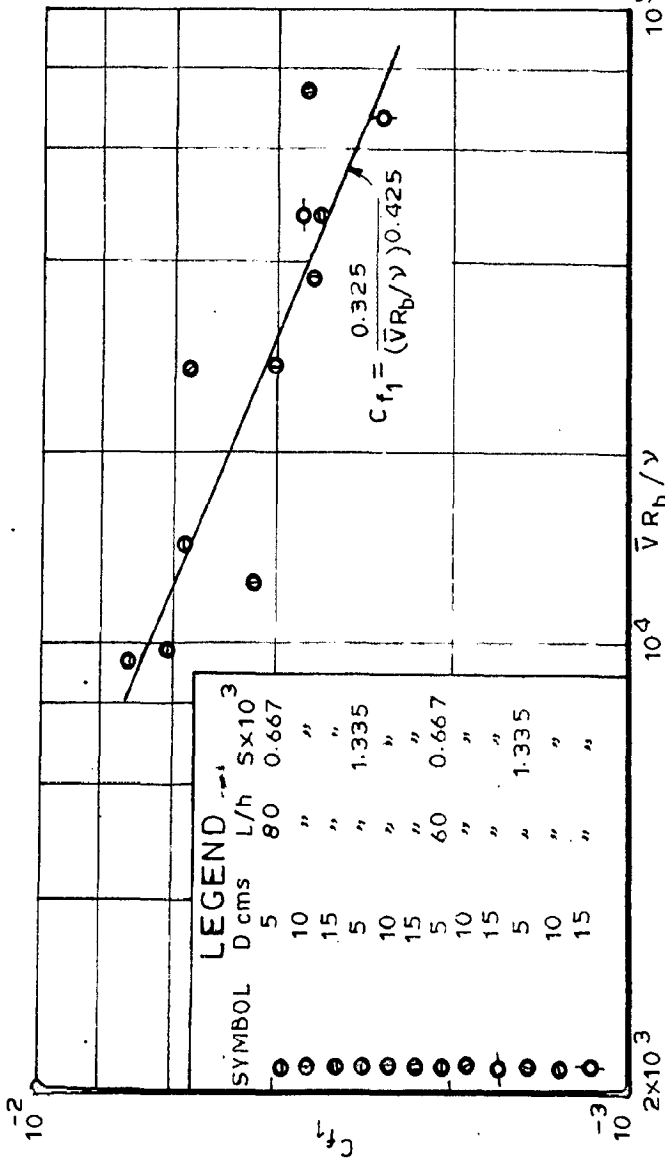


FIG. 5.13 - VARIATION OF C_{f1} WITH \bar{V}_{Rb}/γ FOR ELEMENTS ON SMOOTH BOUNDARY

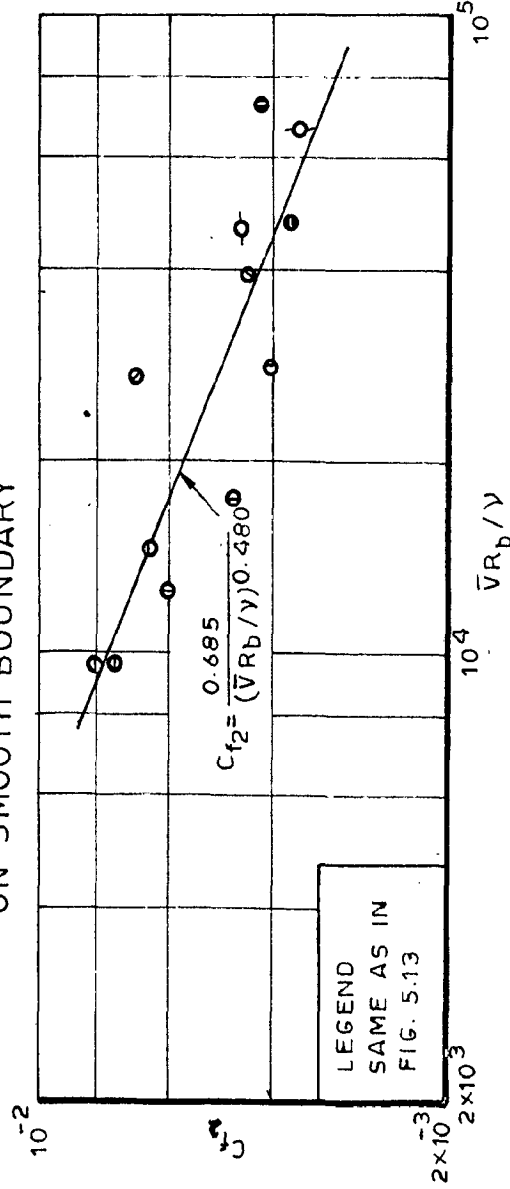


FIG. 5.14 - VARIATION OF C_{f2} WITH \bar{V}_{Rb}/γ FOR ELEMENTS ON SMOOTH BOUNDARY

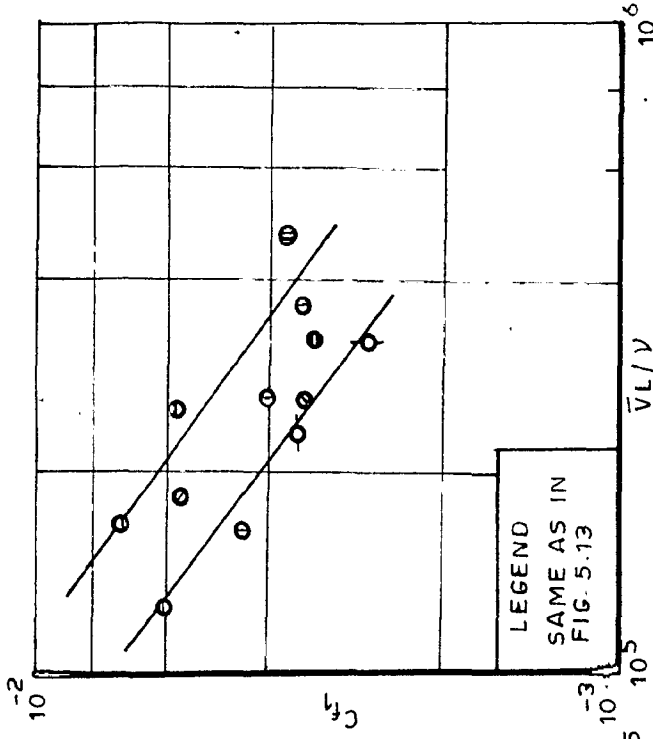


FIG. 5.15 - VARIATION OF C_{f1} WITH \bar{V}_L/γ FOR ELEMENTS ON SMOOTH BOUNDARY

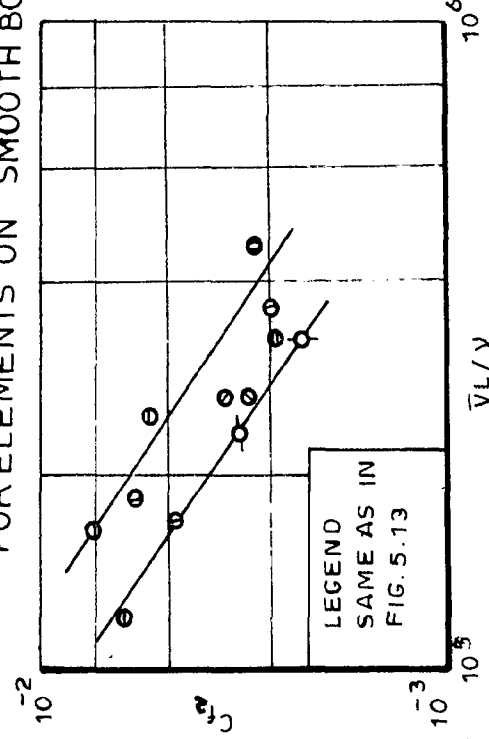


FIG. 5.16 - VARIATION OF C_{f2} WITH \bar{V}_L/γ FOR ELEMENTS ON SMOOTH BOUNDARY

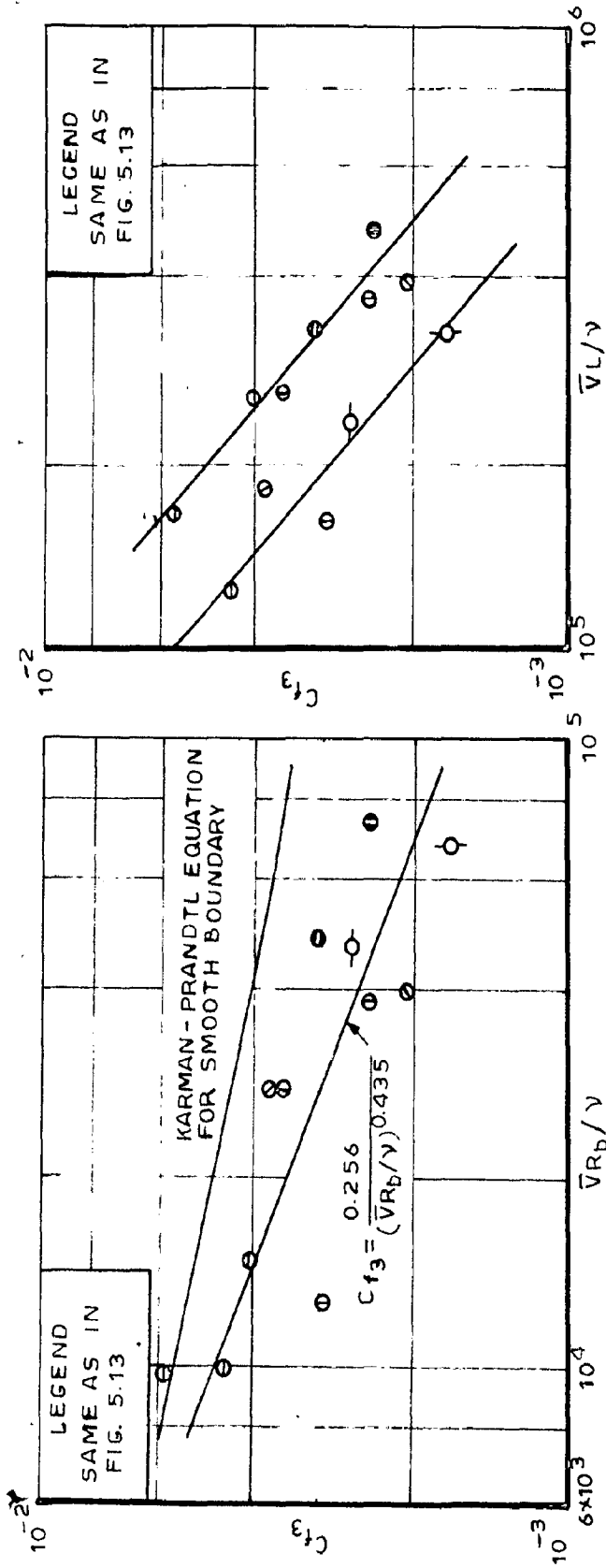


FIG.5.17 - VARIATION OF Cf_3 WITH $\bar{V}R_b/\gamma$ FOR ELEMENTS ON SMOOTH BOUNDARY

FIG.5.18 - VARIATION OF Cf_3 WITH $\bar{V}L/\gamma$ FOR ELEMENTS ON SMOOTH BOUNDARY

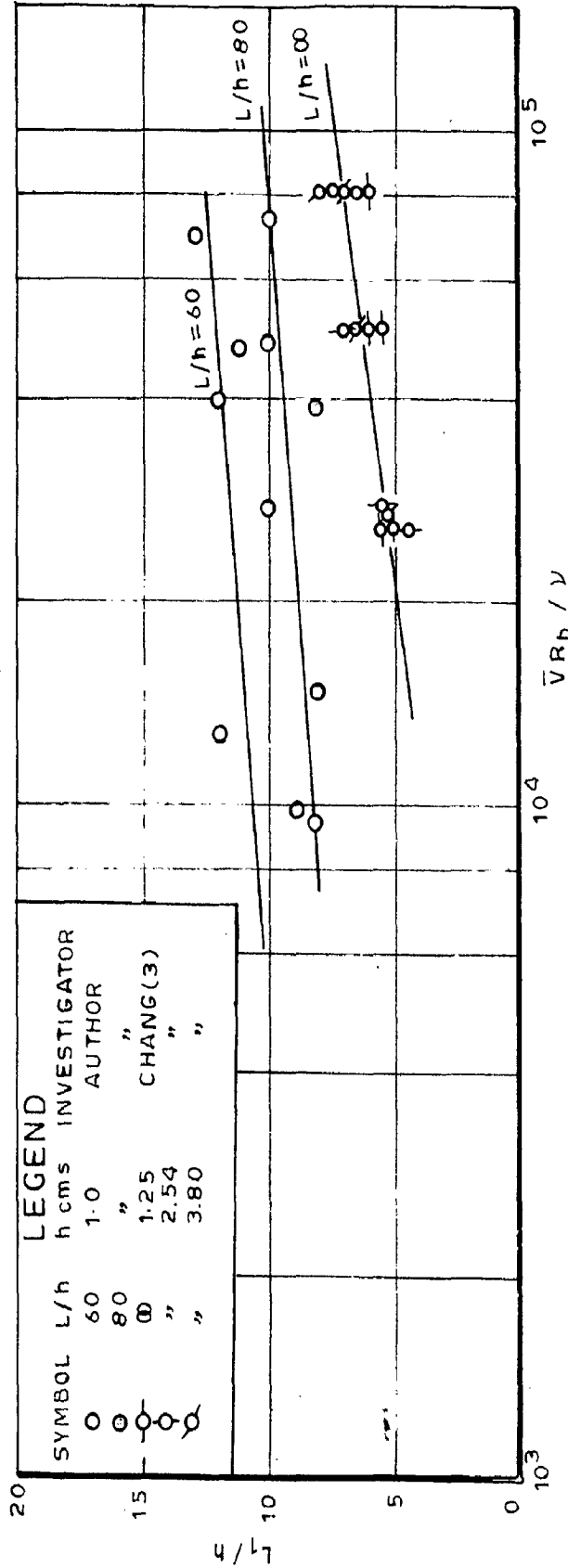


FIG.5.19 - VARIATION OF L/h WITH $\bar{V}R_b/\gamma$ FOR ELEMENTS ON SMOOTH BOUNDARY

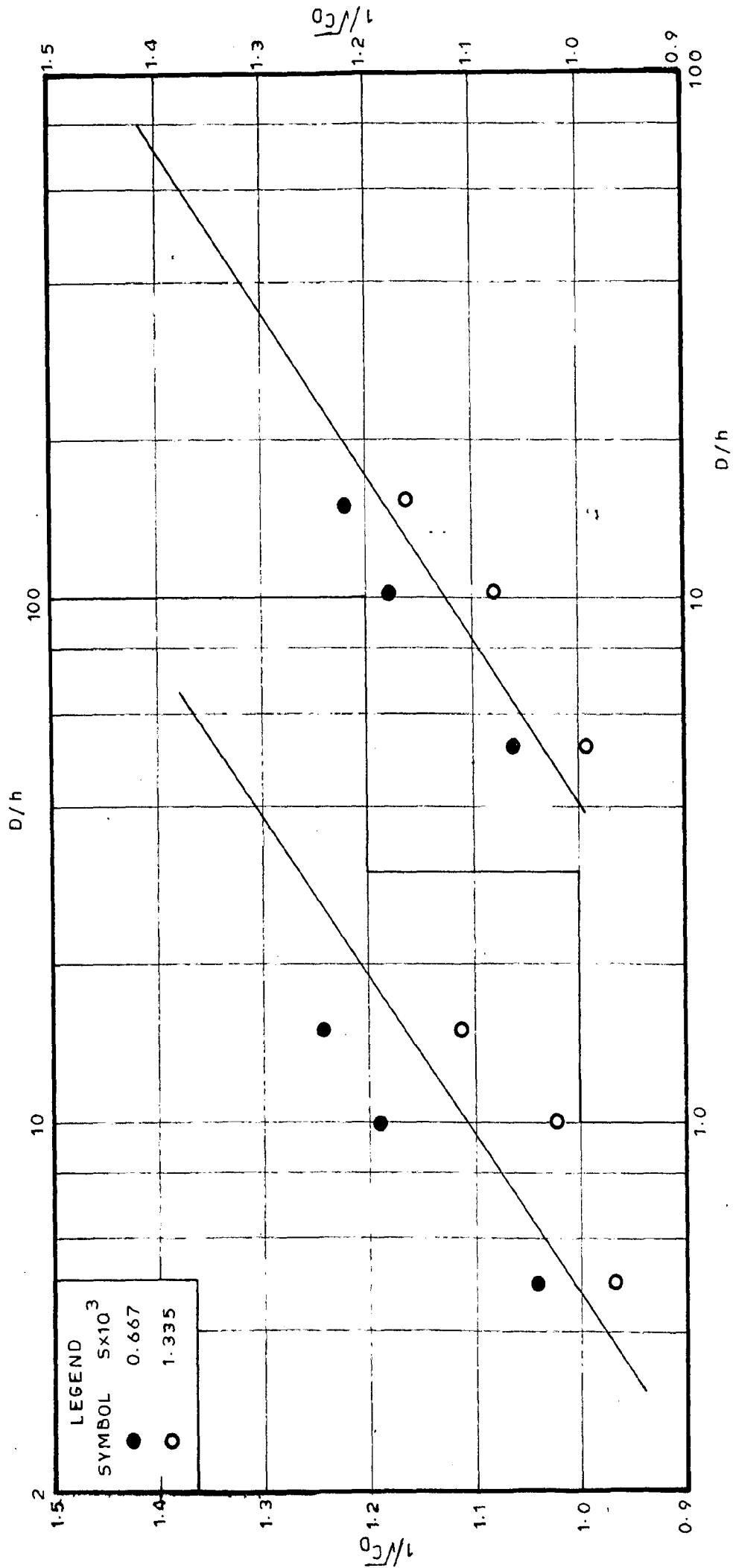


FIG. 5.20 - VARIATION OF $1/\sqrt{C_D}$ WITH D/h AND L/h FOR ELEMENTS ON SMOOTH BOUNDARY

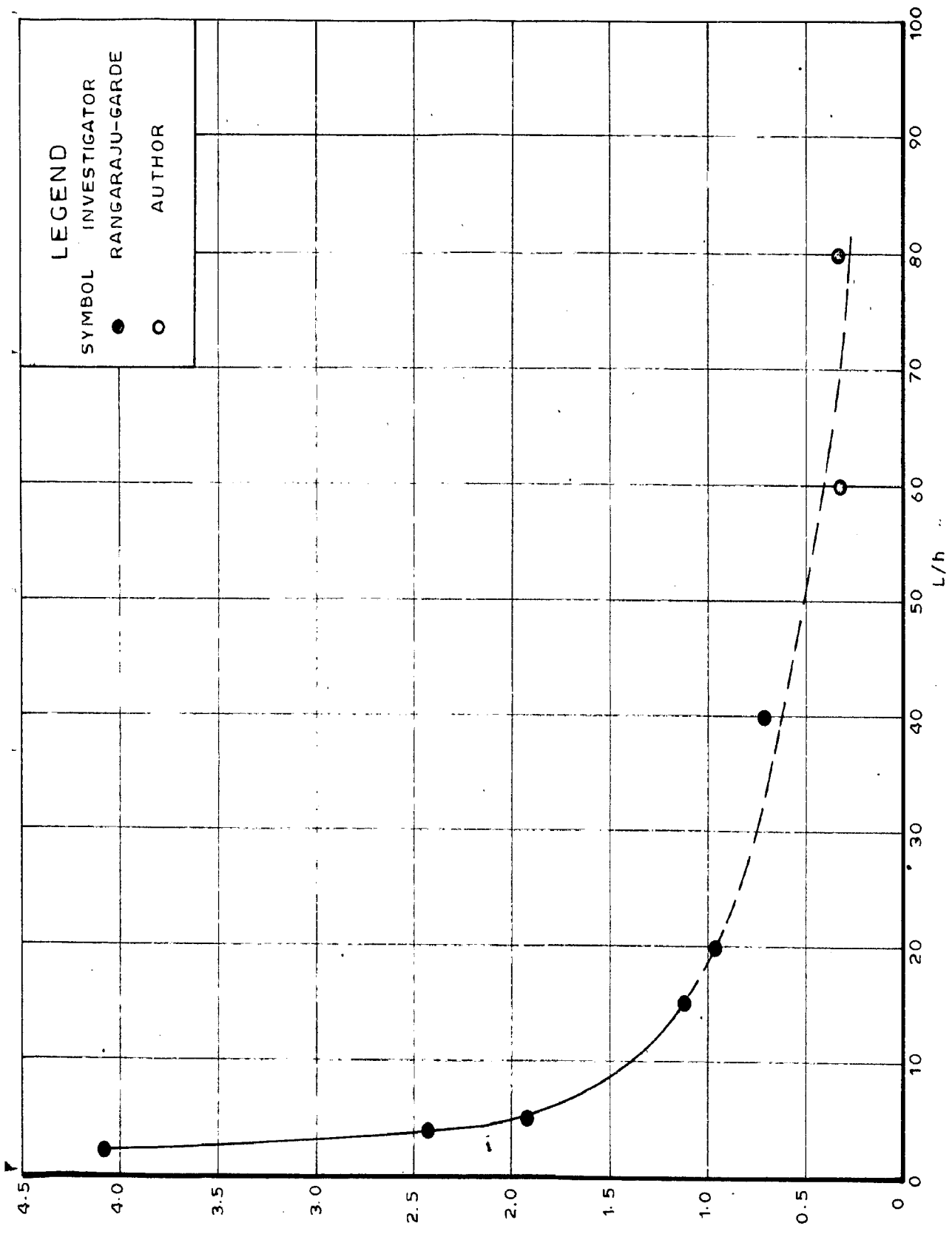


FIG.5.21 - VARIATION OF C1 WITH L/h FOR ELEMENTS ON SMOOTH BOUNDARY

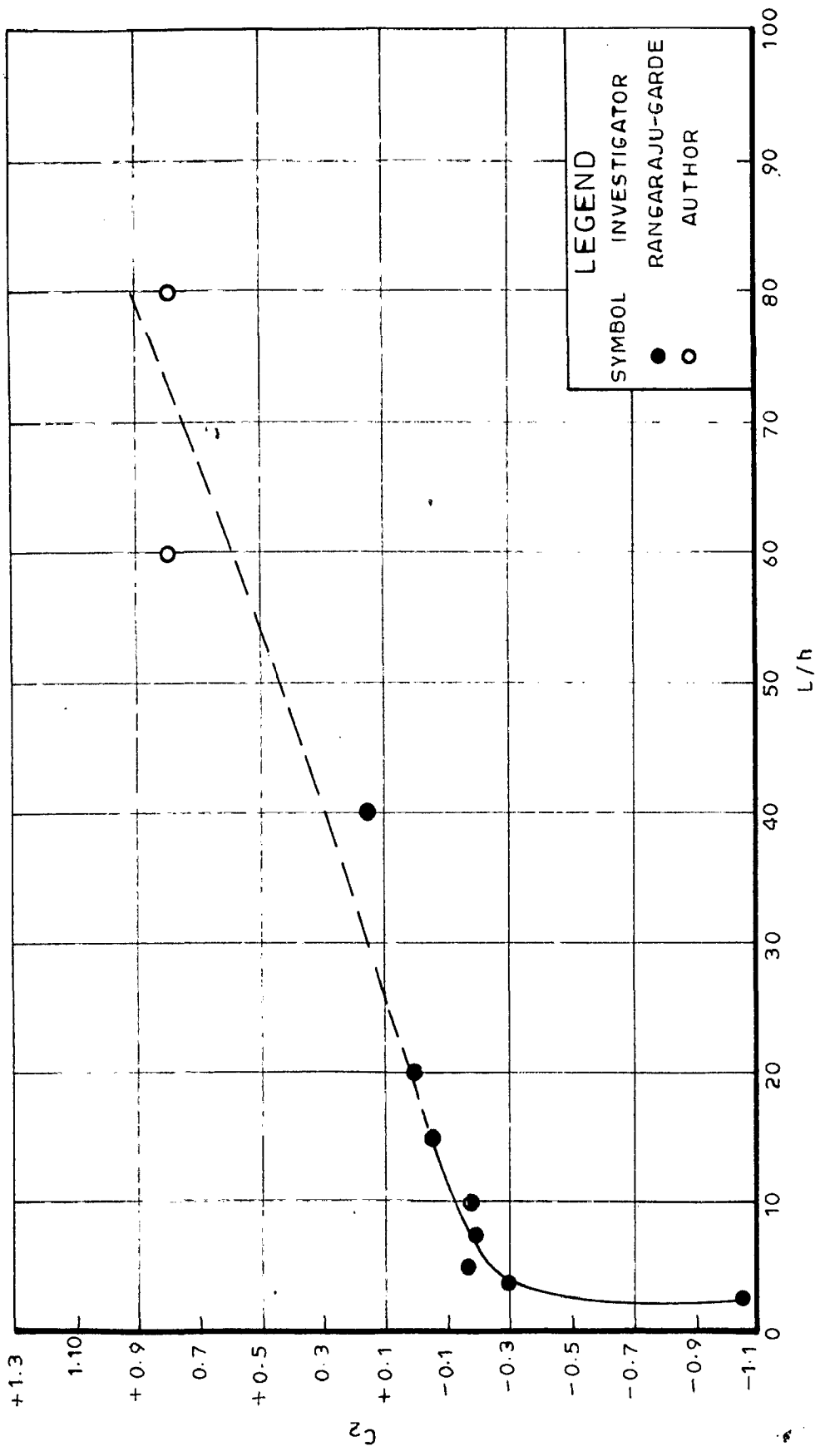


FIG.5.22_VARIATION OF C_2 WITH L/h FOR ELEMENTS ON SMOOTH BOUNDARY

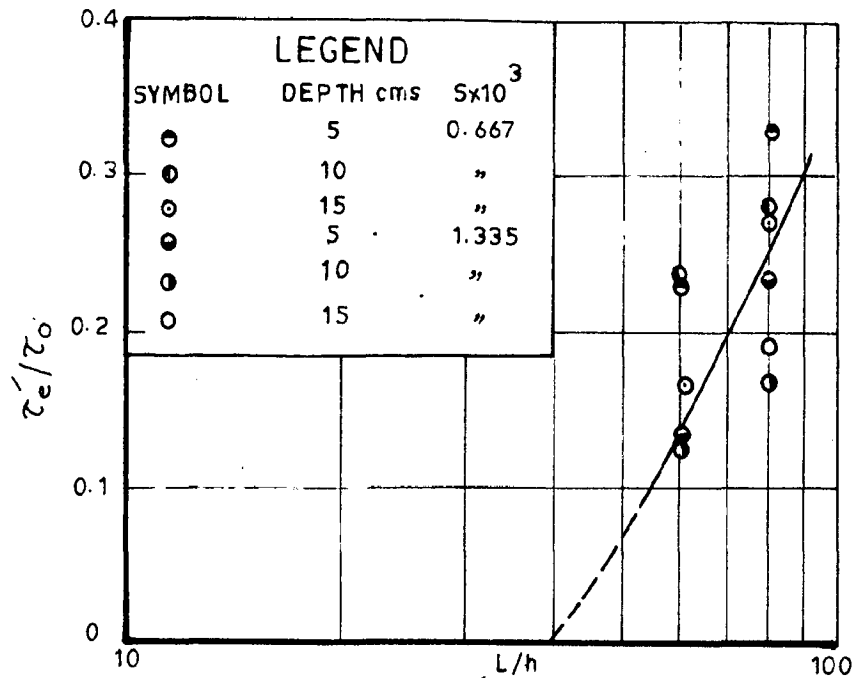


FIG.5.23_VARIATION OF τ_e/τ_0 WITH L/h FOR ELEMENTS ON SMOOTH BOUNDARY

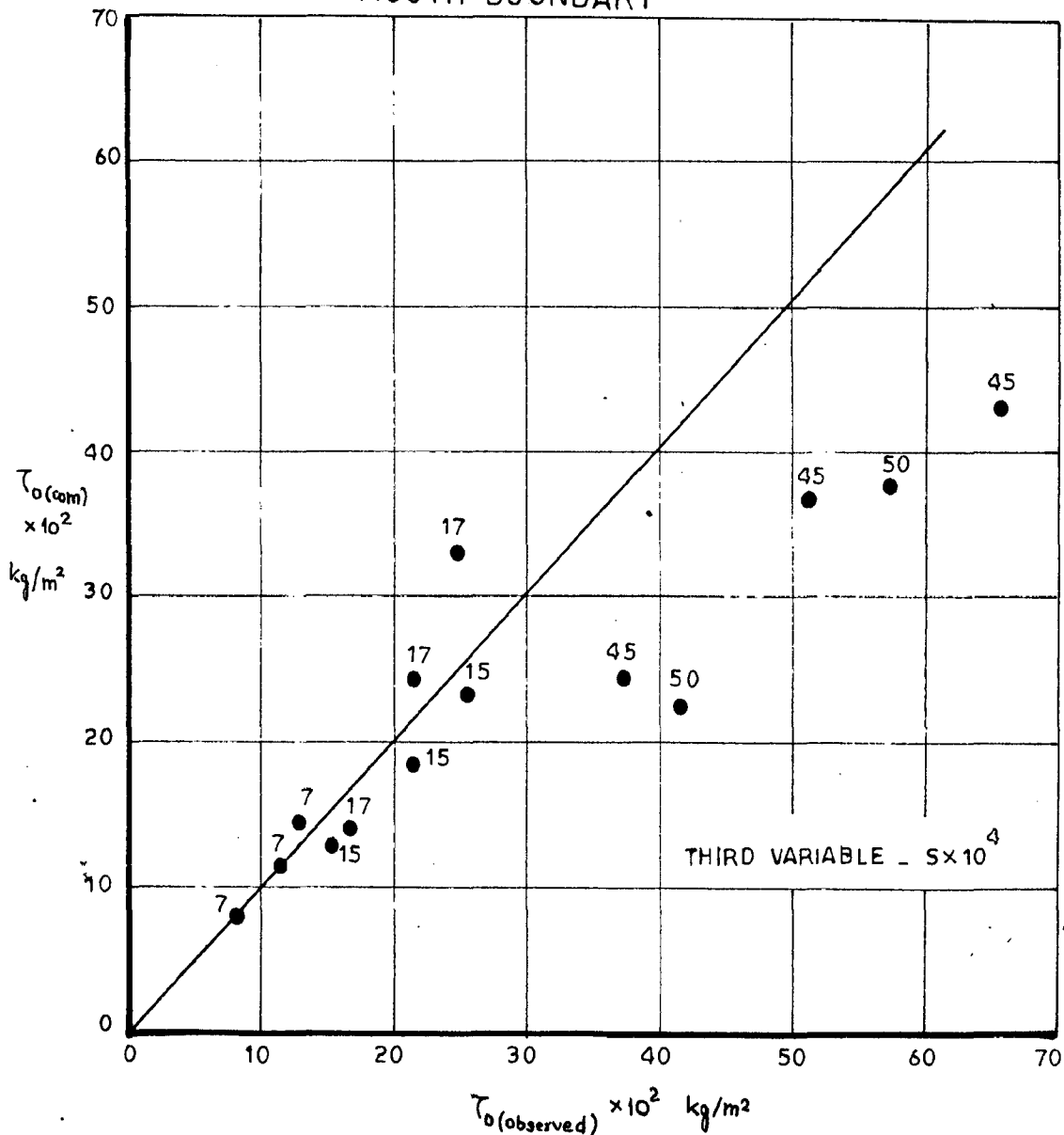


FIG.5.24_PREDICTION OF SHEAR FOR BASHA'S DATA USING AUTHOR'S METHOD

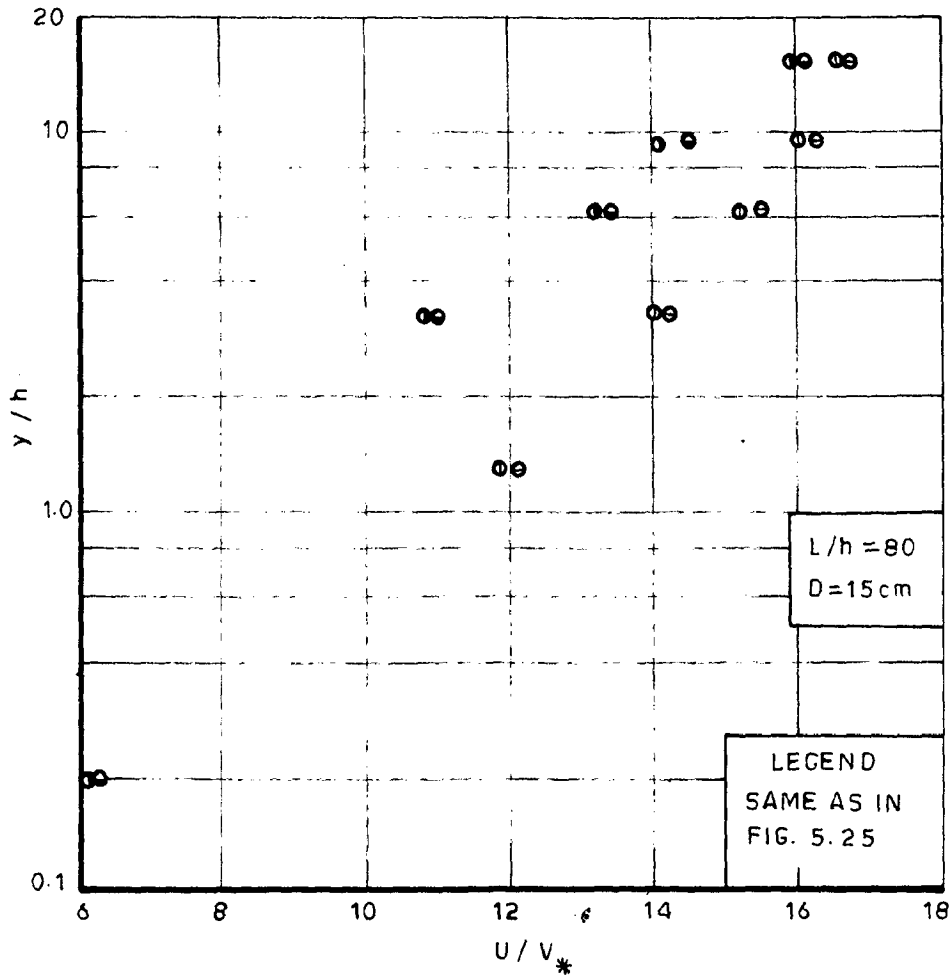
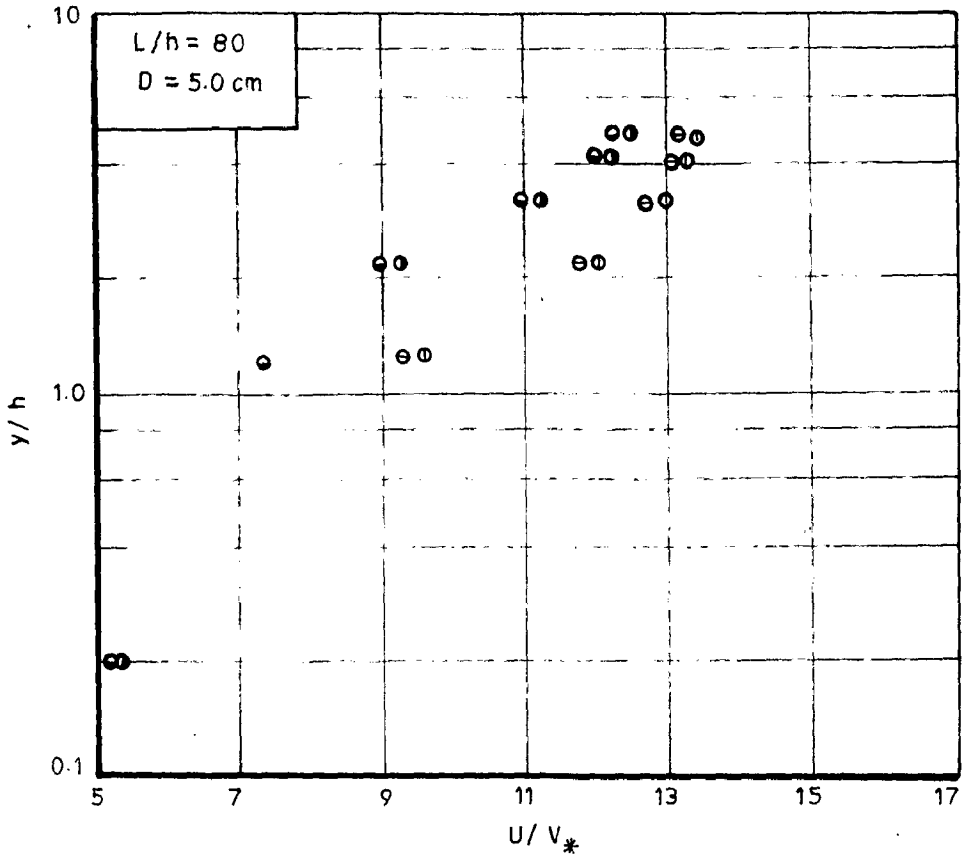


FIG. 5.26. PLOT OF U/V_* VS $\log_{10} y/h$ FOR ELEMENTS ON SMOOTH BOUNDARY

APPENDIX

TABLE - ISUMMARY OF DATA COLLECTED BY THE AUTHOR ON SINGLE ROUGHNESS ELEMENT

Width of the Flume = 47.25 cms.

| Run No. | Cms h | cms D | Cumecs Q | T ^o C | cms/sec V | C _D |
|---------|----------|----------|-------------|------------------|--------------|----------------|
| 1 | 4.0 | 8.30 | 1.20 | 17.5 | 31.30 | 6.60 |
| 2 | 4.0 | 10.10 | 1.50 | 19.5 | 30.90 | 4.50 |
| 3 | 4.0 | 12.00 | 1.70 | 19.0 | 30.11 | 2.81 |
| 4 | 4.0 | 16.01 | 2.25 | 19.0 | 29.82 | 2.26 |
| 5 | 4.0 | 16.01 | 3.00 | 18.0 | 40.00 | 1.81 |
| 6 | 4.0 | 27.27 | 3.35 | 17.5 | 26.05 | 1.47 |
| 7 | 4.0 | 32.00 | 4.80 | 18.0 | 32.21 | 1.32 |
| 8 | 3.0 | 7.50 | 1.00 | 18.0 | 28.25 | 4.27 |
| 9 | 3.0 | 9.00 | 1.25 | 19.0 | 28.80 | 2.91 |
| 10 | 3.0 | 15.01 | 2.50 | 18.5 | 35.60 | 1.98 |
| 11 | 3.0 | 18.00 | 2.85 | 19.5 | 33.73 | 1.63 |
| 12 | 3.0 | 21.10 | 3.14 | 19.5 | 31.40 | 1.23 |
| 13 | 3.0 | 27.03 | 3.70 | 20.0 | 29.20 | 1.18 |
| 14 | 3.0 | 36.02 | 4.70 | 19.5 | 28.21 | 0.814 |

TABLE - II

SUMMARY OF DATA COLLECTED BY THE AUTHOR USING 2-DIMENSIONAL STRIPS ON ROUGH BOUNDARY

Width of the flume = 47.25 cms. Manning's 'n' for glass side wall = 0.009

| Run No. | cms h | cms L | 5 x 10 ³ | cumeccs Q x 10 ³ | cms D | T°C | cms/sec V | Cms R _b | C _D |
|---------|----------|----------|---------------------|--------------------------------|----------|-------------------|--------------|-----------------------|----------------|
| 15 | 4.0 | 160 | 1.0 | 9.8 | 12.86 | 31.0 | 17.10 | 12.20 | 3.50 |
| 16 | 4.0 | 160 | 1.0 | 27.5 | 23.05 | 31.5 | 25.11 | 21.30 | 2.06 |
| 17 | 4.0 | 160 | 1.0 | 51.5 | 32.37 | 32.0 | 33.53 | 28.20 | 1.63 |
| 18 | 4.0 | 160 | 2.0 | 12.9 | 12.85 | 32.0 | 21.30 | 12.10 | 3.70 |
| 19 | 4.0 | 160 | 2.0 | 42.5 | 23.60 | 32.5 | 39.13 | 21.00 | 2.43 |
| 20 | 4.0 | 160 | 2.0 | 72.0 | 32.00 | 32.0 | 47.65 | 27.30 | 1.79 |
| 21 | 4.0 | 80 | 1.0 | 6.9 | 12.50 | 31.5 | 13.10 | 12.10 | 4.35 |
| 22 | 4.0 | 80 | 1.0 | 21.8 | 23.30 | 33.0 | 20.00 | 21.70 | 1.78 |
| 23 | 4.0 | 80 | 1.0 | 43.5 | 35.30 | 32.5 | 26.00 | 31.80 | 1.16 |
| 24 | 4.0 | 80 | 2.0 | 8.9 | 12.80 | 32.5 | 15.50 | 12.40 | 4.53 |
| 25 | 4.0 | 80 | 2.0 | 30.0 | 23.40 | 31.0 | 26.91 | 21.80 | 1.69 |
| 26 | 4.0 | 80 | 2.0 | 66.5 | 36.00 | 31.5 ⁷ | 39.01 | 30.8 | 1.41 |

TABLE - III

SUMMARY OF DATA COLLECTED BY THE AUTHOR USING 2-DIMENSIONAL STRIPS ON SMOOTH BOUNDARY

Width of the flume = 47.25 cms. Manning's 'n' for glass side wall = 0.009

| Run No. | cms h | cms L | cms L ₁ | Sx10 ³ | Cumeqs Qx10 ³ | cms D | T°C | cms/sec V | Cms R _b | Kg/m ² T' x10 ² | Kg/m ² T'' x10 ² |
|---------|----------|----------|-----------------------|-------------------|-----------------------------|----------|------|--------------|-----------------------|--|---|
| 27 | 1.0 | 80 | 8.0 | 0.667 | 4.30 | 5.0 | 26.0 | 18.60 | 4.56 | 1.25 | 1.00 |
| 28 | 1.0 | 80 | 10.0 | 0.667 | 15.80 | 10.0 | 26.0 | 29.61 | 8.30 | 1.80 | 1.57 |
| 29 | 1.0 | 80 | 10.0 | 0.667 | 26.00 | 15.0 | 26.0 | 36.70 | 11.65 | 2.31 | 2.06 |
| 30 | 1.0 | 80 | 8.0 | 1.333 | 6.30 | 5.10 | 27.0 | 26.80 | 4.66 | 2.10 | 1.46 |
| 31 | 1.0 | 80 | 8.0 | 1.333 | 18.00 | 10.00 | 27.0 | 39.15 | 8.37 | 2.72 | 1.88 |
| 32 | 1.0 | 80 | 10.0 | 1.333 | 34.50 | 15.0 | 27.0 | 39.40 | 12.70 | 4.66 | 2.97 |
| 33 | 1.0 | 60 | 9.0 | 0.667 | 4.25 | 5.25 | 26.0 | 18.0 | 4.76 | 1.00 | 0.734 |
| 34 | 1.0 | 60 | 11.0 | 0.667 | 13.20 | 10.30 | 26.0 | 26.80 | 8.77 | 2.08 | 1.390 |
| 35 | 1.0 | 60 | 11.5 | 0.667 | 24.00 | 15.10 | 26.0 | 33.70 | 12.00 | 2.05 | 1.330 |
| 36 | 1.0 | 60 | 12.0 | 1.335 | 5.90 | 5.20 | 28.0 | 24.10 | 4.55 | 1.31 | 0.863 |
| 37 | 1.0 | 60 | 12.0 | 1.335 | 18.50 | 10.40 | 28.0 | 38.00 | 9.00 | 2.60 | 1.500 |
| 38 | 1.0 | 60 | 13.0 | 1.335 | 35.00 | 15.50 | 28.0 | 47.80 | 12.40 | 3.14 | 2.035 |